*Graphical Abstract

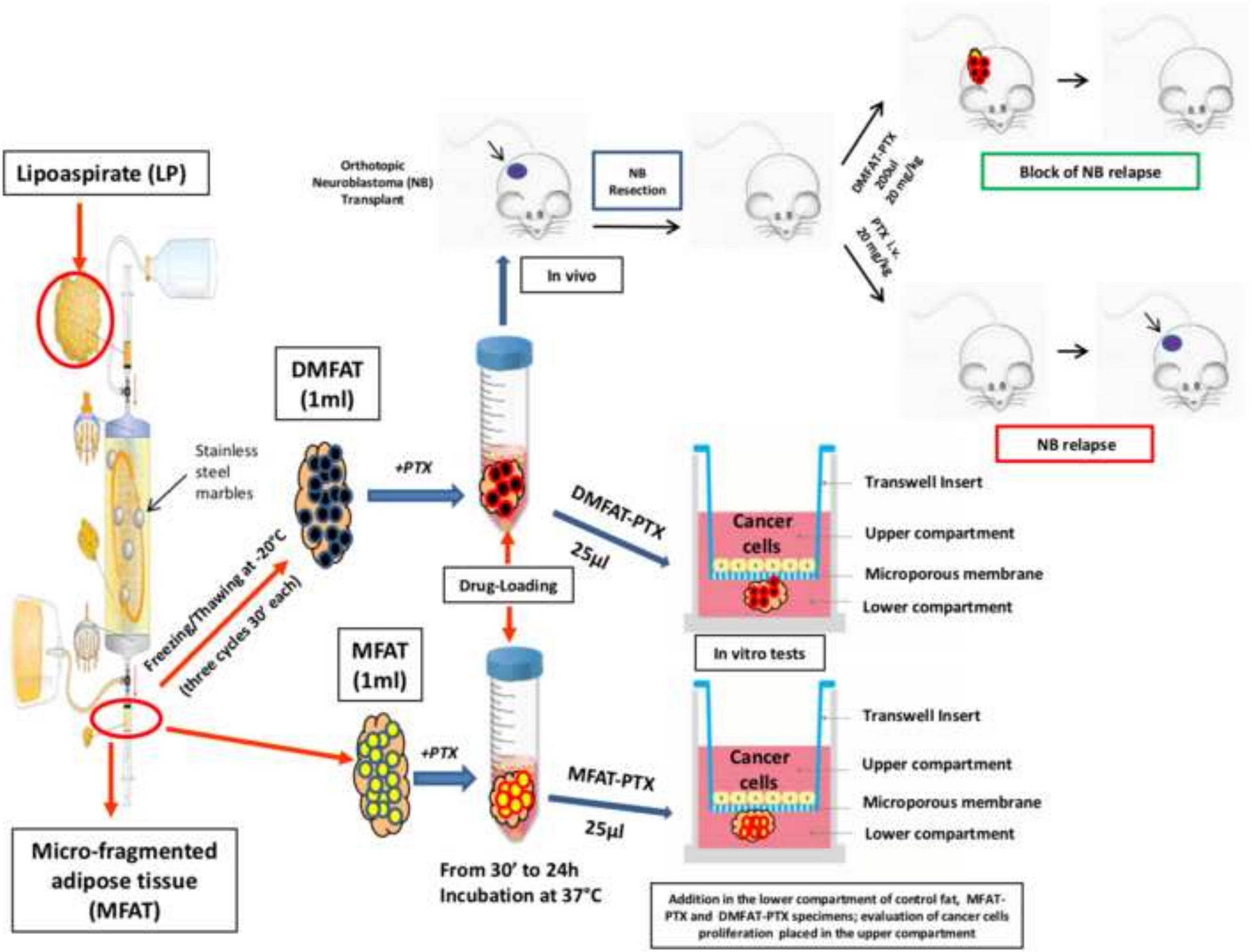

Title: Microfragmented human fat tissue is a natural scaffold for drug delivery: potential application in cancer chemotherapy.

Authors: Giulio Alessandri[1]*^, Valentina Coccè[2], Fabio Pastorino[3], Rita Paroni[4], Michele Dei Cas[4], Francesco Restelli[5], Bianca Pollo[6], Laura Gatti[1] Carlo Tremolada[6,7], Angiola Berenzi[8], Eugenio Parati[1], Anna Teresa Brini[2,9], Gianpietro Bondiolotti[10], Mirco Ponzoni[3^] and Augusto Pessina[2]*^

Affiliations:

1.Cellular Neurobiology Laboratory, Department of Cerebrovascular Diseases, Foundation IRCCS Neurological Institute Carlo Besta, Milan, Italy

2. CRC StaMeTec, Department of Biomedical, Surgical and Dental Sciences, University of Milan, Milan, Italy

3. Laboratory of Experimental Therapy in Oncology, IRCCS Istituto Giannina Gaslini, Genoa, Italy

4.Clinical biochemistry and mass spectrometry lab, Dept. Health Sciences, University of Milan, Milan, Italy

5. Department of Neurosurgery, Foundation IRCCS Neurological Institute Carlo Besta, Milan, Italy

6. Image Institute, University of Milan, Milan, Italy.;

7. School of Healthcare Science, John Dalton Building, Manchester Metropolitan University, Chester Street, Manchester, M1 5GD, UK

8. Section of Pathological Anatomy DMMT, University of Brescia, Brescia, Italy

9. IRCCS Istituto Ortopedico Galeazzi, Milan, Italy

10. Department of Medical Biotechnology and Translational Medicine, University of Milan, Milan, Italy

**These authors contributed equally to this work.*

^ *These authors equally share the rank of last author.*

***# Corresponding author: Giulio Alessandri**: Cellular Neurobiology Laboratory, Department of Cerebrovascular Diseases, IRCCS Neurological Institute C. Besta, Via Celoria 11, 20131 Milan, Italy – giulio.alessandri@istituto-besta.it*

Author for correspondence (e-mail: giulio.alessandri@istituto-besta.it)

Running Title: ***Microfragmented fat tissue for cancer treatment***

Abstract

Localization of chemotherapy at the tumor site can improve therapeutic efficacy and reduce systemic toxicity. In previous studies we have shown that mesenchymal stromal cells (MSCs) isolated from bone marrow or adipose tissue can be loaded with the anti-cancer drug Paclitaxel (PTX) and kill cancer cells when localized nearby. We here investigated the capacity of human micro-fragmented adipose tissue (MFAT), used as a natural scaffold of MSCs, to deliver PTX with the idea to improve local drug concentration and to prolong the therapeutic activity. Surprisingly, we found that both fresh but also devitalized MFAT (DMFAT) (by freezing/thawing procedure) were able to deliver and release significant amount of PTX, killing several human cancer cell lines *in vitro* with a long lasting activity. In an orthotopic mice model of Neuroblastoma (NB) transplant, DMFAT loaded with PTX prevents or delay NB relapse when placed in the surgical area of tumor resection, without any collateral toxicity. We concluded that MFAT, but also DMFAT, may represent very innovative natural biomaterials able to localize and release anti-cancer molecules at the tumor site, helping to fight cancer in human.

Keywords: *Micro-fragmented adipose tissue; Anti-cancer chemotherapy; Drug delivery; Natural scaffold; Biomaterials.*

1. Introduction

Cancer is one of the major causes of death worldwide [**1**]. One of the main treatments of many human cancers is nowadays represented by chemotherapy. However, it is well known that many of the drugs used for the treatment of tumors usually produce harmful side effects to patients, and this aspect is mainly due to their extreme systemic toxicity: the intravenous injection of chemotherapeutics is, in fact, an event having more than one final target.

Chemotherapeutic drugs usually reach cancer cells and, at the same time, healthy tissues and organs [**2, 3**]. It is reasonable to affirm that such harmful effects, sometimes also lethal, could be strongly reduced if the effect of chemotherapy may be more specifically localized at the tumor site. The approaches to reduce side effect of the drug while increasing the therapeutic levels at tumor sites are under deeper investigation. Many studies have long been looking for new approaches to favor anti-cancer drug localization and to develop new "Drug Delivery" (DD) systems [**4, 5, 6, 7, 8, 9**].

Among different methods to improve DD, the use of synthetic polymers as well as natural biomaterials has been recently proposed to enhance anti-cancer therapy efficacy [**10, 11**]. In particular, the use of nano-micrometric nanomaterials as well polymers (both synthetic and natural) are receiving great interest because they can maximize the efficiency of therapeutic treatments, since of their possibility, within the body, to reach the site of a tumor, avoiding to affect healthy tissues with benefit for patients [**9, 10, 11**].

In the last decades, our laboratories have been very active in searching for new DD systems for cancer treatment [**12, 13, 14, 15**]. Specifically, we focused our attention on the use of Mesenchymal Stromal Cells (MSCs) for DD since their extremely high resistance to the toxicity of potent anti-cancer drugs such as Doxorubicin or Paclitaxel (PTX) [**16, 17**]. The MSCs, in our experiments, have been initially isolated from bone marrow. Subsequently, adipose tissue (AT) derived MSCs (AT-MSCs) have been used, given that AT has a rich content of such cells and is an easy obtainable human tissue that requires, to be taken, a minimally invasive surgical procedure.

Despite the therapeutic efficacy that MSCs loaded with PTX (MSCs-PTX), demonstrated *in vitro* and *in vivo* at a preclinical level on various kind of human cancer [**17, 18**], the use of MSCs as well as many other biomaterials used for DD in cancer chemotherapy is still characterized by important translational limitations. Focusing on our approach, firstly, the preparation of MSCs-PTX requires a significant manipulation, that is mandatory to follow the GMP regulations. This procedure implicates high production costs, limiting the possibility to perform repeated treatments and the possible use on a large scale of patients. In addition, since the amount of drug transported by a single MSC is very low (< 1pg/cell), to achieve a potential significant drug concentration at the

tumor site is probably necessary to prepare and to inject several millions (up to 10^8 for single treatment) of MSCs. Finally, in our works MSCs-PTX demonstrated to maintain anti-tumor efficacy only for few days [**17**].

Taking into account of such critical aspects and looking to improve MSCs-PTX anti-cancer activity, we hypothesized that the whole microfragmented AT (MFAT) specimens could work as a scaffold for DD. In fact, the micro-fracture of adipose tissue, although traumatic, does not seem to modify the vascular niche where MSCs reside [**19, 20**]. For our study fat micro-fragmentation was obtained through a commercial device called "Lipogems®",that starting from human Lipoaspirate (LP) results in a homogeneous tissue rich in MSCs content [**19, 20, 21**], easy to manipulate and having an increased surface available to bind molecules.

This idea was also supported by our previous results, investigating the phenotypic and morphological characteristics of MFAT. Indeed, we found that the process of fat micro-fragmentation device leads to obtain a biomaterial that includes and combines a natural structural scaffold organization and a very well preserved stromal vascular fraction (SVF), very rich in MSCs and pericytes [**21**]. To note, MFAT preparations are successfully used in aesthetic medicine as well as in orthopedic diseases [**22, 23**]; moreover, differently from other biological product administrated to patient that requires GMP standards, MFAT requires a lower complex GMP procedure for clinical application [**24, 25**].

Here we demonstrated, for the first time, that fresh preparation of MFAT specimens and, surprisingly, even its devitalized MFAT (DMFAT) counterpart, a fat derivative obtainable through a simple freezing/thawing (F/T) procedure, were very effective in adsorbing and releasing significant amount of the anti-cancer molecule PTX. Both MFAT and DMFAT loaded with PTX (MFAT-PTX; DMFAT-PTX) were able to kill many different human cancer cell lines *in vitro* when located nearby tumor cells, with an impressing long lasting anti-cancer activity. In addition, DMFAT-PTX placed in nude mice at the site of surgical resection of Neuroblastoma (NB) orthotopic xenografts, blocked or delayed tumor relapse, thus confirming its potent anti-tumor activity and suggesting a possible use as a DD tool in the treatment of human cancer.

2. Material and Methods

2.1 Samples collection and Ethics Statements

Samples of LP have been obtained by liposuction of subcutaneous tissue as previously described elsewhere by using disposable cannulas provided with the Lipogems® kit [**24, 25**]. Tissue samples were collected from ten plastic surgery operations after signed informed consent by the patient, in accordance with the Declaration of Helsinki. The approval for their use was obtained from the Institutional Ethical Committee of Milan University (n.59/15, C.E. UNIMI, 09.1115). For all the experiments performed in this study LP was obtained from ten different human donors that underwent plastic surgery (**see supplementary Table 1**).

2.2 MFAT and DMFAT preparation

MFAT specimens were prepared from LP as previously described [**21, 25**]. Briefly, around 50/100 ml of LP was used for MFAT preparation by using a standard 225-ml Lipogems® device (provided by Lipogems® International, Milan, Italy). The LP collected by syringe was pushed into the Lipogems® device through a filter for a first clusters reduction; afterwards, the five stainless steel marbles inside the device are shaken to disaggregate fat material producing cell clusters and micro fragmented fat tissue that migrated to the top of device, while blood contaminating cells and undesired fat residues were removed by a gravity counter flow of saline solution. When the solution inside the device appear yellow and clear, the device was turned up-side down and a second micro-fragmentation of the tissue was obtained by pushing with a syringe the adipose clusters through a size reduction filter. At the end of this procedure, MFAT product was aspirated by a syringe connected with the device and was ready for investigation.

Devitalized MFAT (DMFAT) was obtained following a previous publish procedure [26], with some minor modifications. Briefly, around half of the MFAT volume obtained from LP was transferred in a conical tube and washed with equal volume of PBS three times by centrifugation at 200g × 10 minutes (. After discarding PBS washing solution, MFAT was aspirated with a syringe, transferred in a new tube and undergoing a freeze (-20°C) and thaw (F/T) cycles (usually 3 of 30’ each) that eventually lead to the killing of all the cells in the stromal vascular fraction (SVF). Aliquots of DMFAT were kept at -20°C until use, others were analyzed to verify the absence of cell viability. For this purpose, DMFAT specimens (1-2 ml) after thawing were processed with collagenase (SIGMA St. Louis, Mo, USA) (0.2% w/v) for SVF extraction as previously described [**21, 27**]. Final cell pellets were rapidly suspended in DMEM medium (Gibco, Life Technologies, Monza,

Italy) to investigate cell vitality by Tripan-blue assay . Aliquots of DMFAT were also processed for histological analysis, to confirm that the connective architecture present in the fresh tissue was not altered by F/T process. DMFAT specimens were washed several times (around 10) with PBS by centrifugation (at 200g for 10'each) in order to remove as much as possible all cell debris and the residual presence of membrane proteins and DNA content and then investigated as previously described [**28**] (**see Supplementary Material and Methods**).

Aliquots of DMFAT (1-2 ml) were also seeded in T25 flask and cultured for 5/7 days in of DMEM serum free medium. At the end of incubation, we determined the content of cytokines and growth factors secreted in the conditioned medium (CM) by using multiplex bead-based assays based on xMAP technology (Bio-Plex Human Cytokine 27-Plex Panel; Bio-Plex Human Group II Cytokine 23-Plex Panel; Biorad Laboratories, Hercules, CA, USA). An equal volume of fresh MFAT specimen (from the same human donor) was similarly processed and evaluated to control SVF vitality.

2.3 Chemicals and Reagents

Methanol, isopropanol, acetonitrile and formic acid (all analytical grade) were supplied from Merck (Darmstadt, Germany). Ammonium formate was purchased from Sigma Aldrich (St. Louis, MO, USA) Water was MilliQ - grade. Paclitaxel (PTX) and PTX-D5 were purchased from Cabru (Arcore, Italy). To treat the fat samples a clinical preparation of PTX (stock solution of 6 mg/ml, Fresenius Kabi, Italy) was used. To study PTX localization in fat samples we used FITC-labelled PTX (PTX-F35) that was kindly provided by Dr Varchi G *(Osteoarticular Regeneration Laboratory, Rizzoli Orthopaedic Institute, 40136 Bologna, Italy)* and applied as previously described [**29**].

2.4 Tumor cell lines

The *in vitro* anti-cancer activity of PTX loaded into MFAT and DMFAT was evaluated against: i)the human Pancreatic Adenocarcinoma cell line CFPAC-1 [**30**], maintained by weekly subcultures (1:10) in Iscove complete medium (IMDM) (Euroclone, UK) supplemented with 10% foetal calf serum FCS (Gibco); ii) the human Glioblastoma cell line U87MG [**31**], kindly provided by Dr. Maria Laura Falchetti (*Neurobiology and Cell Biology Institute CNR Rome, Italy*), maintained in RPMI 1640 medium and sub-cultured twice a week (1:5) (Euroclone UK) + 10% FCS; iii) the human, wild type and luciferase (luc) transfected Neuroblastoma (NB) (IMR-32, SH-SY5Y, HTLA-230, NB1691) cell lines, grown in complete DMEM or RPMI-1640 medium, as previously described [**14, 32, 33**]. Cells were tested for Mycoplasma contamination, characterized

by cell proliferation and morphology evaluation, and authenticated at time of experimentation by multiplex short tandem repeat profiling by BMR Genomics (Padova, Italy). All cell cultures were followed and photographed with a Nikon Eclipse TE300 microscope (Nikon, Shinjuku, Japan); cell counts were manually performed with trypan blue coloration technique, supported by Adobe Photoshop Premiere (San Jose, CA, USA).

2.5 Procedure for PTX priming of MFAT and DMFAT specimens

Before PTX priming, MFAT and DMFAT specimens were washed twice with PBS by centrifugation (200g × 10'). Based on our previous procedure used for PTX priming of MSCs [**17**], for each ml of both MFAT or DMFAT specimens, a PTX stock solution (6 mg/ml) diluted in Iscove complete medium (IMDM +10% FBS + 2mM L-glutamine; Euroclone, UK) was added to reach a final concentration of 2 µg/ml. Then, samples were gently shaken and incubated for about 24h (37°C, 5% CO_2). At the end of incubation MFAT-PTX and DMFAT-PTX specimens were washed twice (200g x 10') with PBS to remove unbound drug. To determine the time required by, MFAT and DMFAT to uptake PTX, samples were treated with 2 µg/ml of PTX diluted in IMDM complete medium, agitated by vortex for 1-2 minutes and then incubated for different time (from 5', 30', 1h, 2h to a maximal of 24h at 37°C, 5% CO_2). A similar procedure was also used to establish the minimal effective dose of PTX to prime MFAT and DMFAT specimens. At this regard, fat samples were treated for 2h with different concentrations of PTX (2, 1, 0.5, 0.25, 0.125 ug/ml) diluted in IMDM complete medium. At the end of incubation, fat specimens were washed twice (200g x 10') with PBS to remove unbound drug. Similar volume of control untreated MFAT and DMFAT specimens were similarly processed. At this point both primed and un-primed MFAT and DMFAT specimens were then ready for studying their biological activity (schematic description of PTX priming of MFAT and DMFAT is shown in **Supplementary Figure 1**).

2.6 Evaluation of PTX released by MFAT-PTX and DMFAT-PTX specimens.

To evaluate the amount of PTX released by MFAT-PTX and DMFAT-PTX specimens, we performed a biological dosage of the drug by evaluating the PTX equivalent concentration (p-EC) [**17**]. Briefly, the effect of both free PTX and CM, derived from MFAT-PTX and DMFAT-PTX specimens cultured for 24h (37°C, 5% CO_2) in IMDM complete medium, on tumor cell proliferation was studied in 96 multiwell plates (Sarstedt, Germany) by using as target CFPAC-1 cells. Serial dilutions (1:2) of drugs or CM from treated and control untreated fat specimens were prepared and added to 1,000/100 µl tumor cells. After 7 days of culture at 37°C, 5% CO_2 cell

viability was evaluated by the MTT (3- (4,5-dimethyl-2-thiazolyl)-2,5-diphenyl-2-H-tetrazolium) assay. The inhibitory concentrations (IC) 50 and 90 were determined according to the Reed and Muench formula [**34**], and also by using the linear regression analysis on the dose-response kinetics of the inhibition. The anti-tumor activity of CM from MFA-PTX and DMFAT-PTX were compared to the one of pure PTX and expressed as PTX equivalent concentration (p-EC) according to the following algorithm p-EC (ng/ml) = IC50 PTX x 100/V50 (ul/well) where IC50 PTX is the concentration of pure PTX producing 50% growth inhibition and V50 the respective volume of CM that produce the same inhibition.

2.7 Evaluation of PTX in CM from MFAT-PTX and DMFAT-PTX by HPLC

The presence of PTX and its metabolites in the CM released from MFAT-PTX and DMFAT-PTX was investigated by high performance liquid chromatography (HPLC) [**35**]. Briefly, PTX was measured by a validated HPLC method over the concentration range of 12.5 to 1,000 ng/ml. After addition of cephalomannine (Sigma, St Louis, MO) as internal standard (final concentration 200 ng/mL), 5 ml of CM was extracted on a Bond Elut LRC C-18 solid-phase extraction cartridge (Varian-Harbor City, CA) and, after evaporation to dryness, the samples were reconstituted in 100 µl of mobile phase and analyzed on the chromatographic system (LC-1200, Agilent Technologies, Santa Clara, CA). Chromatographic separation was achieved on a Zorbax RX- C18 analytical column (Agilent Technologies) using a mobile phase containing 48% acetonitrile–52% distilled water. Detection was by UV absorbance at 230 nm. The standard curve was fitted to a weighted (1/Y2) linear regression curve [**35**].

2.8 Localization of PTX adsorbed by MFAT and DMFAT specimens

To study the internalization and localization of PTX into MFAT and DMFAT specimens, a Fluorescent PTX (PTX-F35) was used. MFAT and DMFAT specimens were treated with PTX-F35 (2µg/ml) following the same procedure used for standard PTX (described above). The uptake of PTX-F35 into fat specimens was evaluated at different incubation time (5', 30' 2h, to 24h) and analyzed under Fluorescent microscopy. The uptake of PTX-F35 by the SVF was performed upon priming MFAT and DMFAT with PTX-F35 for 2h, thereafter MFAT and DMFAT were processed with collagenase (as described above) for SVF extraction. The cell pellets were washed two times in PBS and then cultured in IMDM complete medium. The living cells were observed with Fluorescent microscope (TCS SP2 AOBS, Leica, Wetzlar, Germany).

2.9 Evaluation of *in vitro* inhibition of tumor growth by MFAT and DMFAT loaded with PTX

All MFAT-PTX and DMFAT-PTX (2µg/ml) preparations were evaluated for anti-cancer activity either by using trans-well inserts in a co-culture assay with cancer cells, or by evaluating the anti-proliferative activity of their CM obtained upon standard 24h incubation (37°C, 5% CO_2) of the MFAT-PTX and DMFAT-PTX specimens cultured in an equal volume of IMDM complete medium. Untreated MFAT and DMFAT specimens were similarly processed and used as control CM samples.

The direct anti-cancer activity of MFAT-PTX or DMFAT-PTX specimens was tested by using tran-swell inserts (0.4 µm pore size; BD Falcon, NJ, USA). Briefly, a different volume (25, 50, 100 µl) of MFAT-PTX or DMFAT-PTX was seeded in wells (24-multiwell plate) and then covered with 700 µl/well of complete IMDM medium. Around $2x10^3$ CFPAC-1 cells were seeded in 300 µl of medium in the upper compartment of trans-well inserts, then placed in wells. In some experiments fat specimens were located in the upper compartment while cancer cells were seeded in the lower well. After 72h of incubation, the direct effect of fat specimens loaded or untreated with PTX on the tumour cell growth was evaluated by staining the adherent cancer cells with 0.25% crystal violet (Sigma Aldrich, USA) for 10', followed by cell lysing with 0.5 mL of 33% glacial acetic acid. The optical density (OD) of the eluted dye was measured at 550 nm (ChroMate, Awareness technology Inc, CT, USA).

The anti-cancer activity of CM derived from both MFAT-PTX or DMFAT-PTX specimens, was evaluated according to a MTT assay [**36**], or alternatively by counting cancer cells in a 72h proliferation assay [**37**]. In some experiments we also investigated the capacity of CM derived from both MFAT-PTX or DMFAT-PTX specimens to induce cancer cell apoptosis through Annexin V-FITC assay (**see Supplementary Material and Methods**).

2.10 Evaluation of anti-angiogenic properties of MFAT and DMFAT primed with PTX in vitro

The anti-angiogenic potential of different amount of MFAT and DMFAT specimens primed or not with PTX (2µg/ml) or their CM, obtained as described above, was tested on the proliferation of Human Umbilical vein ECs (HUVECs) (purchased from Lonza). ECs phenotypes were routinely maintained in EGM bullet kit plus 10% FCS (Lonza).

HUVECs proliferation assay was performed as described [**38**]. Briefly, HUVECs were harvested from culture flask by trypsin. After enzyme inactivation and centrifugation, cells were re-suspended in EGM medium + 0.2% BSA and counted. To evaluate the growth response to control CM and to PTX primed (2µg/ml) MFAT and DMFAT specimens, 0.5 ml of HUVECs (10^4 cells) were seeded

into each well of a 24-multiwell plate coated with collagen type I; after cell adhesion, medium was aspirated and replaced with EGM complete medium supplemented or not with different dilution (ranging from 1:2 to 1:8) of control CM and primed MFAT-PTX and DMFAT-PTX derived CM. Negative control consisted in the addition of PTX (from 1 to 100 ng/ml), while positive control growth medium consisted in EGM + 10%FCS. After 72h, the wells were washed, fixed and stained. The cells were counted with a calibrated ocular eyepiece in ten different fields at 400X magnification. The capacity of MFAT-PTX and DMFAT-PTX to inhibit HUVECs proliferation was also tested by co-culture assay using trans-well insert as described above for tumor cells. The co-culture assay, using trans-well inserts, between MFAT and DMFAT specimens loaded or not with PTX and HUVECs was performed as described above for CFPAC-1.

2.11 Kinetic of PTX release from MFAT-PTX and DMFAT-PTX

About 1ml of MFAT and DMFAT specimens were treated or not with 2 µg/ml PTX for 2h. After three washes with PBS, control and treated fat specimens were seeded in 5 ml round bottom tube (Falcon) with 1ml of IMDM complete medium (ratio 1:1). After 1 day of culture the CM was collected upon centrifugation (200g x 10') and replaced with fresh medium. This procedure was repeated at 2, 5, 7 days and for 8 weeks (around 2 months) replacing medium every week. At the end of each incubation time the CM was collected and then tested at various dilutions (1:2 until 1:16) on the proliferation *in vitro* of CFPAC-1, IMR-32 and U87MG tumor cell lines, as described above. The total amount of PTX in the CM and the percentage of PTX released from MFAT-PTX and DMFAT-PTX was estimated by the calculation of the p-EC (ng/ml) at each incubation time.

2.12 Kinetic of PTX incorporation and evaluation of PTX saturation dose for MFAT and DMFAT

To evaluate time necessary to upload PTX by MFAT and DMFAT specimens, 1 ml of each specimen was exposed to an equal volume of medium containing 2 µg/ml PTX in a round bottom 5ml tube. PTX loading was performed at different times (5' 30', 2h, 6h and 24h). At the end of each incubation time, samples were centrifuged (200g x 10') and this procedure was followed by two other washes with medium. Washing medium was collected and analysed for the biological dosage and by HPLC analysis to determine the amount of unbound PTX (described above) and to calculate the quantity of PTX carried by MFAT and DMFAT specimens (by subtraction from the total PTX added). Subsequently, a study of MFAT and DMFAT for PTX saturation dosages was addressed. MFAT and DMFAT specimens (1ml) were treated with three progressively increased concentrations of PTX (100, 1,000, and 4,000 µg/ml) for 2h. Then, specimens were washed three

times with PBS and hydrophilic fractions and loaded floating fractions were then analysed by HPLC (procedure described above) to detect unbound and bound PTX, respectively.

2.13 Pharmacokinetic (PK) of PTX released by DMFAT-PTX *in vivo*

Mice were purchased from Envigo (Envigo, Bresso, Italy) and were housed under pathogen-free conditions. Experiments were reviewed and approved by the licensing and ethical committee of Ospedale Policlinico San Martino and by the Italian Ministry of Health (project n.: 661/2016-PR), and in compliance with the "ARRIVE" guidelines (Animals Research: Reporting in Vivo Experiments).

For the PK and biodistribution experiment, 6-weeks-old female immunocompetent BALB/cOlaHsd mice were injected, either subcutaneously (s.c., n = 12) or intraperitoneally (i.p., n=12) with 10 mg/kg of DMFAT-PTX (corresponding at 200 µg PTX in 200 µl of DMFAT). Two, 24, 72 and 168 (7 days) hours post treatment, blood and healthy livers and kidneys from all mice, together with the site of DMFAT-PTX injection from mice treated s.c., were collected and stored until use.

Samples were added with 100 µl of IS (Paclitaxel D5 0.1 µg/ml) then plasma was extracted Solid Phase Extraction (SPE), whereas tissues homogenate (s.c. injection area, liver and kidney) by single-step liquid extraction with methanol/isopropanol/formic acid (60:39.2:0.8). Dry extracts were redissolved with 150 µl of methanol and 10 µl injected in LC–MS/MS analysis.

The analytical system consisted of a UPLC (Dionex 3000 UltiMate) coupled to a AB Sciex 3200 QTRAP instrument with electrospray ionization (ESI) source (AB Sciex S.r.l., Milano, Italy). Separation was attained on a reversed-phase Luna C18(2) column (50 mm x 2, 3 µm) (Phenomenex, CA, USA), with a linear gradient between eluent A (water + 5 mM ammonium formate + 0.1% formic acid) and eluent B (acetonitrile + 0.1% formic acid). The column was equilibrated with 20% (B) for 2 min, increased to 95% (B) in 4 min, held for 0.5 min, back to the initial conditions in 0.5 min and kept for 2 min at 20% (B). The flow rate was 0.4 mL/min, the autosampler and the column oven were kept at 15°C and 30°C, respectively. PTX and PTX-d5 peaks were both eluted at 6 min. The mass analysis was carried out by Multiple Reaction Monitoring (MRM) in positive ion mode (ESI+) by following the transitions: 854 > 286 for PTX and 859 > 291 for PTX-d5. Detailed technical information can be found in the supplementary material and methods.

2.14 Evaluation of *in vivo* anti-tumor activity of DMFAT-PTX

In the first series of experiments, five-week-old Athymic Nude-Foxn1^{nu} mice (Envigo) (n = 5/group) were injected with 1 × 10^6 HTLA-230 NB cells in the left adrenal gland (day 0/ d_0), as previously described [**14,** **39**], and then treated at the days 18, 21, 26 and 33 (reported $T_{1\text{-}4}$), either *i.p.* or *i.v.* with 10 mg/kg of DMFAT-PTX (200 µg PTX/ 200 µl) and free PTX, respectively.

Loading of PTX into just thawed DMFAT specimens were performed 30' before injection adding 1 mg of PTX (around 166 µl of the stock PTX solution 6 mg/ml) to 1 ml of DMFAT and vigorous agitation. Control (CTRL) mice received saline. After orthotopic tumor injection, mice were observed every 2 day to establish tumor appearance and their survival time was followed until died (about 60 days after tumor injection). In a second series of experiments mice were injected with 1 x 10^6 HTLA-230-luc cells in the left adrenal gland (d_0) and then their tumors were surgically resected on day 18 (d_{18}), as previously described [**14, 39**]. Mice were treated after tumor resection and at the days reported (T_{1-5}) with 10 mg/kg of either DMFAT-PTX (n = 5) or free PTX (n = 5). Specifically, the first dose of DMFAT-PTX was lean locally on the site of the tumor immediately after its resection, the other 4 doses were injected i.p. Mice received free PTX i.v. CTRL mice received saline. BLI was performed 2h after tumor resection (d_{18}) and 24h after the last treatment (d_{41}). A similar experiment was also performed injecting IMR-32-luc cells (1×10^6 cells) in the left adrenal gland (d_0) of nude mice and then their tumors were surgically resected on day 14 (d_{14}). Mice were treated after tumor resection with 15 mg/kg of either DMFAT-PTX (n = 14) or free PTX (n = 13), in loco and *i.v.*, respectively. CTRL mice received saline (n = 6). Then, to avoid possible PTX-related toxicity, mice received a second lower dose of treatment (10 mg/kg), either *i.p.* (DMFAT-PTX) or *i.v.* (free PTX) (d_{21}). BLI was performed after tumor resection (d_{14}) and at d_{22}.

2.15 Statistical analysis

The experiments were performed using MFAT e DMFAT samples from a total of 10 human donors investigated (**Supplementary table 1**). Tests were generally run in triplicate and the reported data are expressed as mean ± standard deviation (SD). If necessary, appropriate statistical tests have been performed using GraphPad Software (GraphPad Inc., SanDiego, CA, USA). Statistical analysis was also performed with the Statistical Package for Social Science (SPSS version 13, IBM, NY, USA). Statistical differences were evaluated by the analysis of variance followed by Tukey-Kramer multiple comparison test and by the two-tailed, unpaired Student test. $P \leq 0.05$ was considered statistically significant.

3. Results

3.1 Killing of cellular components by F/T procedure of MFAT specimens

To verify if our F/T procedure abolished all cell viability in MFAT specimens, both control MFAT and DMFAT specimens were digested with collagenase for cells extraction. In contrast to normal fresh MFAT specimens where the total cells recovered ranged from 1.8 to 5.6 × 10^5/ml and the

MSCs were 14 to 78 × 10^3/ml, no living cells, including MSC phenotype, was found in DMFAT after collagenase SVF extraction (**Supplementary Table 1, side A**). In addition, according to the notation that cultured MFAT secretes significant amount of cytokines and growth factors [**21, 28**], the analysis of CM of DMFAT showed a very poor content in cytokines and growth factors (**Supplementary Table 1, side B**).To ensure that our F/T procedure did not alter the original structure of the MFAT (21), histological examination of DMFAT was performed (**supplementary Figure 2**). We found that architecture of fat was not significantly altered by F/T; the structure of the connective (stained for Collagen IV), the adipocyte as well microvascular capillaries (stained with CD31) were well conserved in DMFAT. Because F/T procedure kills the cells, we usually washed 3-4 times with abundant PBS DMFAT specimens to eliminate cell debris and DNA content that remains trapped in the tissue. After this treatment, the amount of proteins and DNA in DMFAT specimens was 0.24±12 µg/ml and 38±18 ng/ml, respectively. A significant reduction of DNA impurities could be obtained by increasing to 10 the number of PBS washes, but this was not sufficient to eliminate all DNA present (around 50% reduction of DNA content was obtained; 38±18 versus 18±13 ng/ml). Anyway, after DMFAT washing, DNA and protein values were significantly lower from those found in fresh MFAT specimens, that was 0.44±0.24 µg/ml for proteins and 45 ± 9 ng/ml for DNA; values similar to those found in our previous study [**28**]. Thus, we concluded that our process of devitalization killed the cells, did not affect significantly the architectural structure and specimens washing only partially reduced both the protein and genetic content.

3.2 MFAT and DMFAT specimens loaded with PTX displayed a potent anti-tumor activity *in vitro*

Based on previous study on MSCs [**17**] we investigated if MFAT could be used to uptake and release PTX and to kill cancer cells in a co-cultured assay. For this purpose, different volume of MFAT-PTX were seeded in trans-well inserts and co-cultured with CFPAC-1, a human pancreatic cancer cell line which we routinely used for its sensitivity to PTX [**40**] (schematic procedure is reported in **Supplementary Figure 1**). An equal volume of untreated MFAT was used as control (**Figure 1**). MFAT-PTX tested at increasing amount of 25, 50, and 100 µl/ml produced a dramatic inhibition of CFPAC-1 proliferation (**Figure 1A**). The lowest amount of sample added to well was enough to produce more than 90% of CFPAC-1 growth inhibition. Then we repeated the same experiments by using DMFAT-PTX to check if MFAT-PTX anti-tumor efficacy was due to its MSCs content. Surprisingly, DMFAT-PTX produced a potent CFPAC-1 growth inhibition and results were practically identical to those obtained with MFAT-PTX (**Figure 1B)**. Even the lowest

volume DMFAT-PTX induced strong cancer growth inhibition, evaluated also by a colorimetric assay (**Figure 1C**). Next, we investigated the efficacy of CM on CFPAC-1 proliferation. We found that the CM derived from all doses of MFAT-PTX (**Figure 1D**) and DMFAT-PTX (**Figure 1E**) owned a potent CFPAC-1 growth inhibition. The anti-cancer activity was dose-dependent and the lowest dose of both MFAT-PTX and DMFAT-PTX released in the CM a PTX-equivalent concentration (p-EC) of around 10 ng/ml, sufficient to completely block CFPAC-1 growth. The p-EC released by MFAT-PTX and DMFAT-PTX did not show significant differences ($p>0.05$) at each volume tested. A very high correlation between the amount of p-EC released and the dose of MFAT-PTX or DMFAT-PTX used ($R^2 = 0.86$ for MFAT-PTX ; $R^2 = 0.75$ for DMFAT-PTX) was observed (**Figure 1F**). CM from control MFAT or DMFAT did not per se affect the proliferation of CFPAC-1 (data not shown).

We then verified if MFAT-PTX and DMFAT-PTX could affect growth of other human cancer cells such as IMR-32 and U87MG, Neuroblastoma (NB) and Gliobastoma (GBM) cell lines, respectively. The CM from MFAT-PTX and DMFAT-PTX was recovered and scalar dilutions were added on cancers cells (**Figure 2**). A potent growth inhibition of IMR-32 cells at each dilution tested, was observed (**Figure 2A**). U87MG cells, that we found very resistant to PTX activity (U87MG IC_{50} was 16 ng/ml versus 2.5 ng/ml of CFPAC-1,) were significantly inhibited (**Figure 2B**). Moreover, the morphological observation of cultured IMR-32 and U87MG cells upon treatment with CM from MFAT-PTX and DMFAT-PTX confirmed the potent anti-cancer activity of CM; besides the significant reduction in cancer cell number, most of the cells, particularly IMR-32, showed necrotic and apoptotic features (**Figure 2C and D).** At this regard a quantification of cancer cell apoptosis by Annexin V expression was performed. As reported in **Supplementary Figure 3** a significant increment in the percentage of Annexin V positive IMR-32 cells was observed, while U87MG cells showed a resistance also to the pro-apoptotic effect of DMFAT-PTX. The dose of 2µg/ml of PTX loaded in MFAT or DMFAT specimens led to a completely block of cancer cells growth. We next evaluated which was the minimal dose of PTX loaded in MFAT and DMFAT for displaying anti-proliferative activity. Both DMFAT-PTX and MFAT-PTX showed a dose-dependent efficacy and a potent cancer cells growth inhibition effect, also at a priming with 0.250 µg/ml PTX. However, both MFAT and DMFAT primed with 0.125 µg/ml PTX were ineffective (**Figure 2E and F**). To note, a trend of less efficacy of DMFAT-PTX versus MFAT-PTX in parallel with the reduction of the PTX loading dosage was observed.

3.3 MFAT-PTX and DMFAT-PTX display a potent *in vitro* anti-angiogenic activity

PTX is an anti-cancer molecule that has been considered an inhibitor of angiogenesis too [**41**]. We thus investigated whether MFAT-PTX and DMFAT-PTX could inhibit angiogenesis *in vitro* (**Figure 3**). We found that doses up to 10 ng/ml were extremely cytotoxic for HUVECs with an IC_{50} ranging from 3.5 to 4.8 ng/ml. The effect of CM from MFAT-PTX and DMFAT-PTX on HUVECs was very cytotoxic at all dilutions tested (**Figure 3A**). To note that at higher concentration (1:2 dilution) even the CM from control DMFAT displayed significant growth inhibition of HUVECs, while CM from MFAT did not substantially affect HUVECs proliferation. Similar results were obtained by co-culture assay using the trans-well inserts (**Figure 3B**). The addition of different volumes of both MFAT-PTX (data not shown) and DMFAT-PTX produced a strong cytotoxic effect on HUVECs (**Figure 3B**).

The morphological analysis of HUVECs cultured in presence of CM from both MFAT-PTX and DMFAT-PTX, showed the presence of cells with nuclear fragmentation a typical feature of apoptosis. (**Figure 3C**).

3.4 *In vitro* long lasting anti-cancer activity of MFAT-PTX and DMFAT-PTX specimens

We next investigated the kinetics of PTX release from MFAT-PTX and DMFAT-PTX specimens. To this end, MFAT-PTX and DMFAT-PTX (primed with 2ug/ml PTX) were cultured in IMDM complete medium and on day 1, 2, 5 and 7 of incubation, CM was aspirated and replaced with fresh one (**Figure 4**). The CM from MFAT-PTX (**Figure 4A**) and DMFAT-PTX (**Figure 4B**) showed a dilution-dependent capacity to inhibit CFPAC-1 growth; no significant differences between MFAT-PTX and DMFAT-PTX were observed. However, the kinetics of PTX released from MFAT and DMFAT showed some difference (**Figure 4C and D**). In particular, after 1 day, the PTX released by DMFAT-PTX was double (p-EC= 124.8 ±15.59 ng/ml) compared to MFAT-PTX (p-EC= 60.98± 5,79 ng/ml). During incubation, the amount of released PTX decreased slowly, but the concentration of PTX derived from DMFAT-PTX was always higher than that released by MFAT-PTX, albeit no statistically significant. Considering the total released PTX during the 7 days of incubation, DMFAT released 302.7±80 ng/ml (15,1% of the total loaded) and MFAT about half, 175.7± 57 ng/ml (8.75% of the total). In general, both MFAT and DMFAT released a constant low percentage of PTX during the first week of culture. To note, the amount of PTX released from MFAT-PTX and DMFAT-PTX every day ranged from 12- to 24-fold and 15- to 48-fold the IC_{50} of CFPAC-1 (2.5ng/ml), respectively; thus, drug concentration in CM, at every time tested, was always highly toxic for CFPAC-1 cells. In summary these data seem to indicate a higher capacity of DMFAT to shed PTX at least during the first 7 days of culture. Similar results were obtained by

using U87MG and IMR-32 cancer cell lines (data not shown). However, in this case we continued to investigate PTX release from MFAT-PTX and DMFAT-PTX for about 60 days. Medium was recovered and replaced every week to determine long-term anti-tumor activity. We found that both MFAT-PTX and DMFT-PTX showed a very long lasting anti-cancer activity against U87MG and IMR-32 cells, with minimal differences (**Figure 4E and G**). During the first 4 weeks the growth of both cancer cell lines was completely blocked by the addition of CM derived from either MFAT-PTX and DMFAT-PTX. During the second 4 weeks of culture, the anti-cancer activity of CM decreased constantly with the time and, even after 8 weeks, CM from both MFAT-PTX and DMFAT-PTX was still very effective: being the proliferation of U87MG and IMR-32 cells reduced of about 50% and 80%, respectively. The analysis of p-EC released in the CM to estimate the kinetics of release of PTX from MFAT-PTX (**Figure 4F**) and DMFAT-PTX (**Figure 4H**) was also evaluated. In summary DMFAT-PTX released a higher amount PTX every week and it was about double of those released by MFAT-PTX. The p-EC trend suggests that MFAT-PTX shed constantly about 7%/week of the total PTX loaded for the first 4 weeks, decreasing to 4% /week for the remaining time. The analysis p-EC secreted by DMFAT-PTX was more variable; 17% of the total was released after one week and then slowly decreased with the time. After 4 weeks about 50% of PTX uploaded was released. To note, after 2 months of culture the percentage of p-EC released by MFAT-PTX and DMFAT-PTX was about 40% and 80% of the total respectively, but the anti-cancer activity of their CM was not significantly different. Finally, the releasing kinetics of PTX from MFAT-PTX and DMFATPTX according to their dilution volume was also investigated (**Supplementary Figure 4**). More precisely, 1ml of MFAT-PTX or DMFAT-PTX (2µg/ml) were cultured for 24h in different volumes of medium (from 1ml to10 ml) and then CM was tested to evaluate p-EC. The percentage of PTX released from MFAT-PTX increased with a good correlation with the dilution volume (R2 =0.91), whereas the release of PTX from DMFAT-PTX was more variable (R2=0.52). The reasons of this difference are not clear. However, the absence of cell vitality in DMFAT seemed to favour PTX release but also the serum albumin, that it is known to have a high affinity for PTX [**42**], may differently affect PTX elution from DMFAT-PTX than from MFAT-PTX.

3.5 Timing of PTX uptake by MFAT and DMFAT specimens

To evaluate the time necessary to uptake the drug, MFAT and DMFAT were primed with PTX (2 µg/ml) for different incubation time. At the end of each incubation time, fat specimens were washed with medium and the unbound PTX was estimated through the biological assay using CFPAC-1 cells for determining p-EC. The amount of PTX retained in MFAT or DMFAT specimens was

estimated by subtracting the unbound p-EC value from the total PTX used (**Figure 5**). We found that the unbound PTX, estimated as p-EC that remain in the washing hydrophilic fraction after only 5' incubation, was 104 ± 49 (ng/ml) for MFAT-PTX and 201 ± 11 (ng/ml) for DMFAT, corresponding to about 5 and 10 % of the total drug used respectively (**Figure 5A**). This means that only 5' of treatment were sufficient to bind most of PTX added to DMFAT and MFAT sample; that was about 90 and 95%, respectively. This result was confirmed by evaluating PTX incorporation in MFAT and DMFAT specimens after prolonged time of incubation (data not shown).

3.6 Localization of PTX uploaded by MFAT and DMFAT specimens

To confirm that PTX can be uploaded very rapidly and to evaluate its possible localization in MFAT and DMFAT specimens, a fluorescent-PTX (PTX-F35), able to label MSCs, was used [**29**]. Incubation with PTX-F35 of MFAT and DMFAT confirmed that few minutes were sufficient for its incorporation. The adipocytes cell component, highly prevalent in both MFAT and DMFAT samples, was able to incorporate most of the fluorescent drug; a deeper analysis of the fluorescence in MFAT confirmed that PTX-F35 was also incorporated by the alive cells present in its SVF compartment, whereas in SVF of DMFAT, as expected, fluorescence was almost completely absent (**Figure 5B**).

To confirm the results obtained with PTX-F35, the SVF from MFAT-PTX was extracted with collagenase, cultured for 24h in medium and its CM tested on CFPAC-1 and IMR-32 to estimate p-EC released. As reported in **Supplementary Figure 5**, CM from SVF isolated from MFAT-PTX (MFAT-PTX-SVF) was effective in a dose-dependent manner in inhibiting both IMR-32 (**Supplementary Figure 5A)** and CFPAC-1 (**Supplementary Figure 5B)**, whereas CM from SVF isolated from DMFAT-PTX (DMFAT-PTX-SVF) did not (data not shown). The evaluation of p-EC released by MFAT-PTX-SVF suggested that only 5% of the total PTX incorporated was present in SVF (**Supplementary Figure 5C**), meaning that the lipid component retained most of the uploaded drug (about 95%) .

3.7 PTX released by MFAT-PTX and DMFAT-PTX maintains its original active structure

A previous study from our group have shown that MSCs-PTX released the drug in its original form [**17**], we therefore investigated if MFAT-PTX and DMFAT-PTX behaved similarly. The HPLC chromatograms obtained from CM from DMFAT-PTX (**Figure 5C**) and from a standard sample of PTX (2 µg/ml) in PBS (**Figure 5D**) showed that a peak of identical retention time of PTX was eluted from both samples. HPLC analysis of CM from MFAT-PTX showed a similar chromatogram

but also revealed the presence of other nonspecific peaks probably due to the secretory activity of SVF as confirmed by the chromatogram of control CM (derived from untreated MFAT) that was similar (data not shown).

3.8 Evaluation of maximal PTX concentration (saturation dose) in MFAT and DMFAT specimens

We next established the "PTX *saturation dose*" is the maximal concentration of PTX that MFAT or DMFAT can uptake. To this end, three very high concentrations of PTX 100, 1,000, 4,000 µg /ml were used (**Supplementary Figure 6**). Results showed that the dose of 1,000 µg of PTX was about the saturation dose for 1 ml DMFAT (**Supplementary Figure 6A**). Indeed, the total PTX extracted was about 96% (961 ± 23 µg /ml) of that uploaded. Increasing doses of PTX to 4,000 µg /ml of DMFAT did not substantially increase the total PTX eluted, that was about 32.3% (1,295 ± 332 µg /ml) (**Supplementary Figure 6B**); the analysis of PTX incorporated by MFAT showed that the saturation dose of PTX /ml was similar, but with high variability among different fat donors, likely due to the variability of cells content from donor to donor (data not shown) [**28**].

3.9 Anti-tumor effects of DMFAT-PTX in an orthotopic animal model of Neuroblastoma

Based on the *in vitro* results, we then investigated the capacity of DMFAT-PTX to affect the growth of cancer cells *in vivo.* For these experiments, only DMFAT specimens were used, because of the advantage given by the possibility to conserve frozen biomaterials until use in mice. We initially decided to verify the potential anti-cancer activity of DMFAT-PTX using the NB cancer cell line HTLA-230. This cancer cell line together with the NB cell line IMR-32 have demonstrated *in vitro* to be very sensitive to PTX activity if compared to other NB cell lines investigated (**Supplementary Table 2**). In addition, in a 3D test using Matrigel as a matrix support, proliferation of HTLA-230 cells was highly inhibited by co-culture with DMFAT-PTX; the expression of MIB-1 marker of proliferation was also highly reduced (**Supplementary Figure 7**).

In a first series of experiments mice (n = 5/group) were injected with $1x10^6$ HTLA-230 cells in the left adrenal gland day 0 (d_0) and then treated, at the days reported (T_{1-4}), either *i.p.* or *i.v.* with 10 mg/kg of DMFAT-PTX and free PTX, respectively. CTRL mice received saline (**Figure 6**). Both treatments did not substantially affect the growth of HTLA-230, when compared to CTRL (**Figure 6A**). Since this experiment indicated that the i.p. injection of DMFAT-PTX in mice bearing well established tumors was not effective, in a second set of experiments a resected model of NB was used (**12**). Therefore, mice were injected with $1x10^6$ luciferase (luc)-transfected HTLA-230 cells

(HTLA-230-luc) in the left adrenal gland (d_0) then their tumors were surgically resected on day 18 (d_{18}) and mice were treated as described in M&M section. Under this schedule of treatments, compared to control mice, DMFAT-PTX blocked HTLA-230-Luc relapse, which was only delayed in mice treated with free PTX (**Figure 6B**).

We next investigated the capacity of DMFAT-PTX to affect the relapse of IMR-32 NB cells given its high sensitivity to PTX (**Supplementary Table 2**). Mice were injected with 1×10^6 IMR-32-luc cells in the left adrenal gland (d_0) and then their tumors were surgically resected on day 14 (d_{14}). Mice were treated after tumor resection with 15 mg/kg of either DMFAT-PTX (n = 14) or free PTX (n = 13), in loco and *i.v.*, respectively. CTRL mice received saline (n = 6). About 69% free PTX-treated mice died for toxicity within 48h after the first treatment. To note, about 20% of mice locally treated with DMFAT-PTX died for respiratory problems related to the high volume of biomaterials injected. Thus, the remaining mice received a second dose of free PTX and DMFAT-PTX at lower dose of 10 mg/kg (d_{21}). Since the rapid relapse in CTRL mice, BLI was performed after tumor resection (d_{14}) and on day 22 (d_{22}). We found that IMR-32-relapse in mice treated with DMFAT-PTX was almost completely blocked. This result is not significantly different compared to that obtained in mice treated with free PTX due only to the small number of animals belonging to this therapeutic group and survived from the first dose of PTX-related toxicity (n=4). (**Figure 6C**).

3.10 Pharmacokinetics (PK) of PTX delivered by DMFAT-PTX

The PK of free PTX has been widely studied elsewhere [**43-44**], here we finally investigated the PK of PTX delivered by DMFAT (**Figure 7**). Blood concentrations of PTX found at 2h were 1,90 ± 0.94 µg/ml (*i.p.*) and 0,27 ± 0,05 µg/ml (*s.c.*), whilethe circulating drug resulted very low (ranging from 0.002 to 0,01 µg/ml) after 24 , 72 and 168h. Plasmatic concentration of DMFAT-PTX after *i.p*. injection at 2h was compatible with PTX value of 2x T1/2 already described [**37**], while the plasmatic level PTX after DMFAT-PTX *s.c.* injection was 86% lower. The values of the apparent volume of distribution at 2h (Vd_{2h}) were 105,2 ml (*i.p.*) and 716,8 ml (*s.c.*) (**Figure 7A**). As expected, after the subcutaneous injection of DMFAT-PTX, the circulatory level of PTX was lower than after *i.p.* injection, indicating a better bio-distribution in tissues. Similarly to blood, the level of PTX found in liver and kidney was higher (3,6 - 5,2 fold) when DMFAT-PTX was inoculated *i.p*. than that administrated *s.c*.. At 2h, the amount of PTX in liver was of 45,90 ± 10,32 µg/gr (*i.p*) versus 12,35 ± 3,00 µg/gr (*s.c.*) corresponding to 22,6% and 6,15% of the total amount of PTX injected respectively. In the kidney we found 26,54± 5,15 µg/gr (*i.p.*) versus only 3,84± 0,40 µg/gr (s.c.) corresponding to 13,2% e 1,9 % of the drug administered, respectively. In summary, when

DMFAT-PTX was given *s.c.* the amount of PTX bioavailable for liver and kidney was reduced to 73 % and 86 % respectively, if compared to the *i.p.* route. (**Figure 7B**).

Although of the technical difficulty to recover all DMFAT-PTX biomaterials, the analysis of the residual amount of drug at the site of injection after 2h was 490,75 ± 161,01 µg/ gr (about 50 % of the injected amount of 1 mg/gr). This concentration decreased significantly at 24h (49,63 ± 9,21 µg/gr) and 72h (18,00 ± 12,46 µg/gr). At 7 days 3.3 ± 1.6 µg/gr of PTX was found, a local drug concentration that must be considered of pharmacological importance, since higher than the IC_{50} for many different cancer cells (**Figure7B**).

At the end, the area under the curve (AUC) was calculated. The $AUC_{2\text{-}168h}$ for plasma showed that the drug availability in plasma after DMFAT-PTX *s.c.* treatment was significantly lower 0,16 µg/ml/days versus the value of 0,98 µg/ml/days observed after *i.p.* treatment.

$AUC_{2\text{-}168h}$ for kidney and liver, upon *s.c.* treatment, was the 17% and 39% respectively of AUC upon *i.p.* treatment. The AUC of residual amount of PTX after *s.c.* treatment (412 µg/day) was about 2,400 time higher than that found for plasma (0.17 µg/day) (**Figure 7C**). All these data, confirmed that DMFAT-PTX given *s.c.* produced a dramatic high local concentration with a minor degree of PTX systemic concentration in respect to *i.p* DMFAT-PTX injection.

4. Discussion

The majority of anti-cancer compounds are cytotoxic for patients because they do not affect only cancer cells but also normal healthy ones. To reduce such undesired side effects, is nowadays clear that a more specifically localized chemotherapy is required [**45, 46**]. To this end, a wide range of biomaterials (both natural and synthetic), able to work as reservoirs and to locally release anti-cancer drugs, are under intense investigation [**9, 47, 48**].

Among several technical approaches that have been studied and used to implement DD specifically at the tumor site, our group and others have demonstrated that MSCs [**17, 49**] derived from AT, but also from other human tissues, can be very effective in delivering anti-tumor agents. In fact, we have shown that MSCs-PTX, when localized at tumor site, can inhibit primary tumor growth [**17**] and even metastases when i.v. administered [**50**].

Despite of such interesting pre-clinical results, the application of MSCs in clinic has raised some concerns, mostly regarding technical procedures for their preparation: i) large number of cells required (up to 10^8 cells) for single treatment, ii) the necessity of GMP conditions for *in vitro* MSCs manipulation and, therefore, very high costs for their production.

Since AT is very rich in MSCs [**51**] and because we evidenced that a micro-fragmented fat derivative, the MFAT, was even more enriched in these cells [**21, 28**], we hypothesized that MFAT specimens per se could be used for anti-cancer DD. Importantly, the MFAT specimens here used were prepared through a closed sterile system (Lipogems® device) that does not require GMP conditions for its clinical applications [**25**].

Based on this premise, we here investigated the anti-cancer capacity of MFAT loaded with PTX. The choice of using PTX was not only based on our previous experience in MSCs priming, but also on the fact that PTX has been shown to owe a strong lipid affinity [**52**], suggesting that MFAT specimens may quickly incorporate this drug. To validate our hypothesis, we also investigated in parallel the behavior of DMFAT specimens, the devitalized form of MFAT, that would be the ideal control of MFAT activity, given that it is only depleted of SVF vitality (including its MSCs content). To note, the procedure that we applied for MFAT devitalization was simple, fast (90' total), easy to perform and was based on three F/T cycles (30'each), a slightly different method from previous reports [**26**], but very effective in killing any cell in the SVF, as we confirmed by the lack of cells vitality, paracrine activity in all DMFAT preparations that here were used. In addition, DMFAT preparations were washed with PBS by centrifugation several times in order to remove as much as possible all cells debris and genetic material that remain trapped inside. (**Supplementary Table 1**).

In summary we found that: a) MFAT, but also its DMFAT derivative, demonstrated an equivalent and efficient capacity to upload PTX; they both incorporated very rapidly PTX (5'were sufficient to incorporate 90% to 95% of added PTX) that was mostly localized in their adipocytes/lipid content; b) they both slowly release PTX efficiently in its original form (no other metabolites were present) and this secretion was prolonged for at least 2 months after priming with a percentage of PTX released by DMFAT that was even double of those released by MFAT; c) both MFAT-PTX and DMFAT-PTX specimens, when co-coltured with cancer cells, or even their CM added to culture medium of many different human cancer cell lines, demonstrated to strongly affect cell proliferation in a dose-dependent manner. They both showed a long lasting anti-proliferative activity *in vitro* (up to 2 months) and similar inhibition of angiogenesis; d) in an orthotopic animal model of human Neuroblastoma (NB), the local administration of DMFAT-PTX at tumor site after its surgical resection reduced NB relapse; e) PK studies demonstrated that PTX delivered by DMFAT (*s.c.*) produced a high local concentration with a significant reduction of PTX systemic concentration, when compared to DMFAT-PTX administered systemically (*i.p.*).

Our results, taken together, strongly support our initial hypothesis, proposing MFAT as a natural biomaterial able to absorb and transport chemotherapeutic drugs. Surprisingly, also the devitalized derivative worked efficiently, leading to the conclusion that the presence of MSCs in the MFAT was not essential to determine its ability to uptake and release the drug and to kill cancer cells. On the contrary, the presence of the adipocytes/lipid content in both MFAT and DMFAT specimens appeared fundamental to permit a quickly uptake of PTX at very high and significant levels: around 1 mg of PTX for 1ml of both MFAT and DMFAT specimens could be uploaded. The uptake capacity of fat biomaterials may clearly depend on the hydrophobic PTX molecules properties (indeed localization of PTX-F35 was mostly found in the adipocytes component), suggesting that other similar lipophilic anti-cancer drugs, such as Vincristine and Vinblastine, may behave similarly.

SVF of MFAT, and probably its MSCs content, seem anyway important to determine a gradual and slower release of PTX. The total weekly amount of drug released by DMFAT was constantly doubled if compared to those released by MFAT, both at early and after prolonged incubation time. To this regard, the active role of MSCs in delaying PTX clearance from MFAT-PTX specimens is supported by our recent data, showing that MSCs in MFAT specimens cultured for long period of time (2 months) in a serum-free medium survived and maintained a secretory activity; in contrast, ECs, or other cells of the SVF did not survive more than few days [**28**].

The amount of PTX released by MFAT and DMFAT was positively correlated with the dose of PTX priming. Interestingly, we observed that a significant amount of PTX (about 125 ng/ml) was adsorbed by MFAT and DMFAT and probably never released (no anti-tumor activity was detected in the CM), suggesting that a quote of PTX may remain entrapped in fat specimens.

So far, it has been shown that fat tissue and, in particular, adipocytes may adsorb and inactivate anti-cancer drugs such as Daunorubicin and Doxorubicin, reducing their cytotoxicity in cancer microenvironments, and lowering anti-tumor effect and survival outcomes [**53-56**]. Our data clearly supports these experimental and clinical evidences and, from a toxicological point of view, shed a new light on the role of AT in controlling anti-cancer drug toxicity that, independently of its capacity to induce drug inactivation, may also act like a "pure drugs reservoir". This occurrence *in vivo* remains to be clarified and it is mandatory to address the role of different fat depots (subcutaneous versus visceral) in drug metabolism and absorption [**55, 56**]. This may also help to understand the causes that lead to organ specific toxicity by some chemotherapeutic agents in cancer patients [**57**].

In vitro our data strongly demonstrated the potent anti-cancer activity of MFAT-PTX and DMFAT-PTX when co-cultured with many different human cancer cell lines. We particularly focused on NB

cell lines with the idea of validating our *in vitro* data, performing *in vivo* experiments in a clinically relevant orthotopic animal model of human NB [**12, 39**]. More precisely, as a proof of concept, we evaluated the anti-NB activity of DMFAT loaded with PTX when administered locally at the tumor site or systemically, through *i.p.* injections. Substantially, the *in vivo* data here reported showed that the treatment of well established tumors with DMFAT-PTX did not affect NB growth, whereas, when DMFAT-PTX was located in the surgical area of tumor resection, a potent effect to inhibit or retard NB relapse was obtained. In addition, if compared to treatment with free PTX, a significant lower systemic toxicity was observed with DMFAT-PTX. To note, the dose of 10 mg PTX /kg, free or uploaded in DMFAT, here used was established based on clinical studies in humans [**58**]. Finally, the preliminary PK and biodistribution studies here reported demonstrated the capacity of DMFAT biomaterial to significantly retain PTX at local site, reducing its hematological concentration and organs biodistribution, as well as its capacity to locally release PTX.

In our opinion, these results may open important new insights regarding the use of AT in cancer chemotherapy. AT is a well known natural biomaterial widely used in many fields of medicine, widening from cosmetic surgery to regenerative and therapeutic medicine [**23-25**]. Fat has been investigated for therapeutic activity either as natural biomaterial but also upon its de-cellularization [**59**]. In particular, in regenerative medicine, decellularized AT (DAT) has been proposed to be used per se given its ability to provide a tridimensional scaffold structure that retains extracelluar matrix components and growth factors necessary for tissue regeneration [**60**]. However, to our knowledge, no studies applied DAT biomaterial for anti-cancer DD. We here did not use DAT but we used a particular AT preparation, MFAT and its devitalized counterpart (DMFAT) obtained through a process of microfragmentation that preserves the cellular and the natural scaffold structure integrity of the original AT [**20, 21**]. To note, AT processed to obtain DAT depleted cells and lipid efficiently, but it also destroy the normal stromal fat architecture **[61**], making DAT an interesting biomaterial for tissue regeneration but its efficiency in PTX delivery remains to be investigated.
Local delivery of anti-cancer drugs is under deeper investigation and can be realized with an impressive number of approaches [**9**]. Focusing on PTX delivery, for example, copolymers [**62, 63**] and natural polymers [**64**] have been studied and used with some efficacy in a translational setting. To establish the real *in vivo* efficacy of MFAT and DMFAT as biomaterials for anti-cancer DD, further experiments are needed. In particular, it will be important to understand the mechanism of how fat biomaterials release PTX and, possibly, other similar drugs. At this regard, since MFAT and DMFAT behave similarly, only a minimal active participation of MSCs P-glicoprotein-related mechanisms to eject drugs, can be claimed [**17, 65**]. Another important aspect that will need to be further elucidated *in vivo* will be the determination of a dose-response activity of MFAT-PTX and

DMFAT-PTX, their capacity to continue DD over longer periods of time and the distance of drug diffusion when they are located in tumors or nearby cancer cells.
Nevertheless, this is the very first study that shows the strong anti-tumor efficacy *in vitro* and *in vivo* of MFAT and of its devitalized form when used as scaffold to deliver the anti-cancer drug PTX, a molecule widely used for the treatment of many different human cancers [**66**].

In conclusion, we think that our results can open new hopes for cancer patients. More precisely, given that: a) MFAT and DMFAT can be easily prepared at low cost, according to minimal consolidated GMP regulations; b) MFAT and DMFAT can be rapidly loaded with significant amount of drug, slowly released in active form for several days; c) MFAT or DMFAT loaded with drugs can be prepared and transplanted during the surgical removal of a tumor; d) DMFAT can be conserved under freezing conditions (–80°C) for long periods of time and thaw before drug loading; we therefore believe that MFAT or DMFAT, once demonstrated effective on a wider *in vivo* experimentation in animals bearing tumors, can be applied for a local chemotherapy of many human cancers. Actually, we do not know if DMFAT, can potentially lead to immunorejection when transplanted *in vivo* due to the insufficient removal of cellular debris and genetic materials [**67**]; moreover, we did not investigated the *in vivo* anti-cancer activity of fresh MFAT-PTX because of the difficulty to have, on the same day, the collection and preparation of MFAT from a human donor and the operated animals ready for treatment.

However, the use of both MFAT and DMFAT for local cancer treatment will open very interesting perspectives for autologous and even heterologous applications in a wide variety of human cancers among which ovarian, mammary, prostatic, pancreatic, hepatic, brain (i.e. Glioblastoma) and, not least, NB patients may beneficiate.

5. Conclusions

Localization of chemotherapy only at the tumor site represents one of the major goal in actual cancer chemotherapy research. We here asked whether MFAT specimens per se could be used for DD of PTX, a potent and widely used anti-cancer drug in human. As a control of MFAT activity, we also investigated DMFAT, a devitalized form of AT, in which SVF cells, including its MSCs content, were killed by F/T procedure. We here, for the first time, clearly demonstrated that both MFAT and DMFAT work as natural biological scaffolds, able to adsorb and release a very significant amount of PTX and to efficiently kill cancer cells both in vitro and in vivo; in an orthotopic animal model of human NB the local administration of DMFAT-PTX at tumor site after its surgical resection blocked or delay NB relapse. We concluded that MFAT, but also DMFAT,

may both represent very innovative natural biomaterials able to localize and release anti-cancer molecules at the tumor site, opening very interesting perspectives for heterologous applications in human cancers.

Author Contributions

Conceived and designed the experiments: GA,AP. Performed the experiments: F.P., FR, MD, FB, VC, AB, ATB, GB, BP (istlogia) LG (apoptosis), . Analyzed the data: AP, GA, RP, F.P., MP, EP. Contributed reagents/materials/analysis tools: CT, FP, MP, EP, GA. Wrote the paper: GA, AP. Supervised of studies: GA, AP.

Funding: *This research was supported by: a) Italian Ministry of Health (Ricerca Corrente to GA, IRCCS Neurological Institute C. Besta Foundation) Rome, Italy; b) Lipogems® International S.p.A*, Milan. Italy; c) CRC StaMeTec, UNIMI Fund RV.RIC.AT16RWEIN02.Milan, Italy*

*The funder had no role in study design, data collection and analysis, decision to publish, or preparation of the manuscript.

Acknowledgments

This manuscript is dedicated in memory of our beloved friend and colleague Anna Benetti.

We thanks: Moris Cadei, Tiziana Gulotta and Lucia Fontana (*Section of Pathological Anatomy DMMT, University of Brescia, Brescia, Italy)*, Ciusani Emilio (*Laboratory of Clinical Investigation, Foundation IRCCS Neurological Institute Carlo Besta, Milan, Italy),* Chiara Calatozzolo (Department of Neuropathology, Foundation IRCCS Neurological Institute Carlo Besta, Milan, Italy), and Loredana Cavicchini (*Department of Biomedical, Surgical and Dental Sciences, University of Milan, Milan, Italy)* who gave a great contribution to technical work execution.

Competing Interests:

Carlo Tremolada is the President and founder of Lipogems International SpA.

All the other Authors have declared that no competing interests exist.

Data availability

The raw/processed data required to reproduce these findings cannot be shared at this time as the data also forms part of an ongoing study.

References

1. Wordwide cancer incidence statistics, http://www.cancerresearchchuk.org/health-professional/cancer-statistics/wordwide-cancer/incidence (Cancer Research UK), 2014.
2. R.T. Skeel, S.N. Khleif, Handbook of Cancer Chemiotherapy, Lippincott Williams & Wilkins, Philadelphia, 2011.
3. M. Barton-Burke, G.M. Wilkes, K. Ingwersen, Cancer chemotherapy Care Plans Handbook, Jones & Bartlett learning, Sudbury, third ed., 2002.
4. O.G. Scharovsky , L.E. Mainetti, V.R. Rozados, Curr Oncol 16 (2009) 7-15.
5. W.M. Saltzman, L.K. Fung, Polymeric implants for cancer chemotherapy, Adv Drug Deliv Rev 26 (1997) 209-230.
6. I. Sousa, F. Rodrigues, H. Prazeres, R.T. Lima, P. Soares, Liposomal therapies in oncology: does one size fit all?, Cancer Chemother Pharmacol 82 (2018) 741-755.
7. A. Cox, P. Andreozzi, R. Dal Magro, F. Fiordaliso, A. Corbelli, L. Talamini, et al., Evolution of Nanoparticle Protein Corona across the Blood-Brain Barrier, ACS Nano 12 (2018) 7292-7300.
8. S. Mahajan, A. Patharkar, K. Kuche, R. Maheshwari, P.K. Deb, K. Kalia, et al., Functionalized carbon nanotubes as emerging delivery system for the treatment of cancer, Int J Pharm 548 (2018) 540-558.
9. K. Krukiewicz, J.K. Zak, Biomaterial-based regional chemotherapy: Local anticancer drug delivery to enhance chemotherapy and minimize its side-effects, Mater Sci Eng C Mater Biol Appl 62 (2016) 927-942.
10. Y. Cheng, C. He, J. Ding, C. Xiao, X. Zhuang, X. Chen, Thermosensitive hydrogels based on polypeptides for localized and sustained delivery of anticancer drugs, Biomaterials 34 (2013) 10338-10347.
11. R. De Souza, P. Zahedi, C.J. Allen, M. Piquette-Miller, Polymeric drug delivery systems for localized cancer chemotherapy, Drug Deliv 17 (2010) 365-375.
12. F. Pastorino, D. Di Paolo, F. Piccardi, B. Nico, D. Ribatti, A. Daga, et al., Enhanced antitumor efficacy of clinical-grade vasculature-targeted liposomal doxorubicin, Clin Cancer Res 14 (2008) 7320-7329.

13. A. Corti, F. Pastorino, F. Curnis, W. Arap, M. Ponzoni, R. Pasqualini, Targeted drug delivery and penetration into solid tumors, Med Res Rev 32 (2012) 1078-1091.
14. I. Cossu, G. Bottoni, M. Loi, L. Emionite, A. Bartolini, D. Di Paolo, et al., Neuroblastoma-targeted nanocarriers improve drug delivery and penetration, delay tumor growth and abrogate metastatic diffusion, Biomaterials 68 (2015) 89-99.
15. M. Ponzoni, F. Curnis, C. Brignole, S. Bruno, D. Guarnieri, L. Sitia, et al., Enhancement of Tumor Homing by Chemotherapy-Loaded Nanoparticles, Small (2018) e1802886.
16. A. Pessina, M. Piccirillo, E. Mineo, P. Catalani, L. Gribaldo, E. Marafante, et al., Role of SR4987 stromal cells in the modulation of doxorubicin toxicity to in vitrogranulocyte-macrophage progenitors (CFU-GM), Life Sci 65 (1999) 513–523.
17. A. Pessina, A. Bonomi, V. Coccè, G. Invernici, S. Navone, L. Cavicchini, et al., Mesenchymal stromal cells primed with paclitaxel provide a new approach for cancer therapy, PLoS One 6 (2011) e28321.
18. S. Pacioni, Q.G. D'Alessandris, S. Giannetti, L. Morgante, I. De Pascalis, V. Coccè, et al., Mesenchymal stromal cells loaded with paclitaxel induce cytotoxic damage in glioblastoma brain xenografts, Stem Cell Res Ther 6 (2015)194.
19. B. Vezzani, I. Shaw, H. Lesme, L. Yong, N. Khan, C. Tremolada, et al., Higher Pericyte Content and Secretory Activity of Microfragmented Human Adipose Tissue Compared to Enzymatically Derived Stromal Vascular Fraction, Stem Cells Transl Med (2018) Sep 26 [Epub ahead of print].
20. F. Bianchi, M. Maioli, E. Leonardi, E. Olivi, G. Pasquinelli, S. Valente, et al., A new nonenzymatic method and device to obtain a fat tissue derivative highly enriched in pericyte-like elements by mild mechanical forces from human lipoaspirates, Cell Transplant 22 (2013) 2063-2077.
21. V. Ceserani, A. Ferri, A. Berenzi, A. Benetti, E. Ciusani, L. Pascucci, et al., Angiogenic and anti-inflammatory properties of micro-fragmented fat tissue and its derived mesenchymal stromal cells, Vasc Cell 18 (2016) 3.
22. A. Bouglè, P. Rocheteau, M. Hivelin, A. Haroche, D. Briand, C. Tremolada, et al., Micro-fragmented fat injection reduces sepsis induced acute inflammatory response in a mouse model, Br J Anaesth (2018) 1e11.
23. O. Zeira, S. Scaccia, L. Pettinari, E. Ghezzi, N. Asiag, L. Martinelli, et al., Intra-Articular Administration of Autologous Micro-Fragmented Adipose Tissue in Dogs with Spontaneous Osteoarthritis: Safety, Feasibility, and Clinical Outcomes, Stem Cells Transl Med (2018) Jul 23 [Epub ahead of print].

24. C. Tremolada, C. Ricordi, A.I. Caplan, C. Ventura, Mesenchymal Stem Cells in Lipogems, a Reverse Story: from Clinical Practice to Basic Science, Methods Mol Biol 1416 (2016) 109-122.
25. C. Tremolada, V. Colombo, C. Ventura, Adipose tissue and mesenchymal stem cells: State of the art and Lipogems technology development, Curr Stem Cell Rep 2 (2016) 304-312.
26. E. Rossi, J. Guerrero, P. Aprile, A. Tocchio, E.A. Kappos, I. Gerges, et al., Decoration of RGD-mimetic porous scaffolds with engineered and devitalized extracellular matrix for adipose tissue regeneration, Acta Biomater 73 (2018) 154-166.
27. R. De Siena, L. Balducci, A. Blasi, M.G. Montanaro, M. Saldarelli, V. Saponaro, et al., Omentum-derived stromal cells improve myocardial regeneration in pig post-infarcted heart through a potent paracrine mechanism, Exp Cell Res 316 (2010) 1804–1815.
28. S. Nava, V. Sordi, L. Pascucci, C. Tremolada, E. Ciusani, E. Zeira, et al., Long lasting anti-inflammatory activity of human micro-fragmented adipose tissue (in press Stem Cell International , 2019).
29. S. Duchi, P. Dambruoso, E. Martella, G. Sotgiu, A. Guerrini, E. Lucarelli, et al., Thiophene-based compounds as fluorescent tags to study mesenchymal stem cell uptake and release of taxanes, Bioconjug Chem 25 (2014) 649-655.
30. J.C. McIntosh, R.A. Schoumacher, R.E. Tiller, Pancreatic adenocarcinoma in a patient with cystic fibrosis, Am J Med 85 (1988) 592.
31. M.J. Clark, N. Homer, B.D. O'Connor, Z. Chen, A. Eskin, H. Lee, et al., U87MG decoded: the genomic sequence of acytogenetically aberrant human cancer cell line, PLoS Genet 6 (2010) e1000832.
32. M. Loi, D. Di Paolo, M. Soster, C. Brignole, A. Bartolini, L. Emionite, et al., Novel phage display-derived neuroblastoma-targeting peptides potentiate the effect of drug nanocarriers in preclinical settings, J Control Release 170 (2013) 233-241.
33. D. Di Paolo, D. Yang, F. Pastorino, L. Emionite, M. Cilli, A. Daga, et al., New therapeutic strategies in neuroblastoma: combined targeting of a novel tyrosine kinase inhibitor and liposomal siRNAs against ALK, Oncotarget 6 (2015) 28774-28789.
34. L.J. Reed, H. Muench, A Simple Method of Estimating Fifty Per Cent Endpoints, Am J Epidemiol 27 (1938) 493–497.
35. L. Gianni, C.M. Kearns, A. Giani, G. Capri, L. Vigano, A. Lacatelli, et al., Nonlinear pharmacokinetic of paclitaxel and its pharmacokinetic/pharmacodynamics relationships in humans, J Clin Oncol 13 (1995) 180–190.

36. T. Mosmann, Rapid colorimetric assay for cellular growth and survival: application to proliferation and cytotoxicity assays, J Immunol Methods 65 (1983) 55–56.

37. M.P. Schiariti, F. Restelli, P. Ferroli, A. Benetti, A. Berenzi, A. Ferri, et al., Fibronectin-adherent peripheral blood derived mononuclear cells as Paclitaxel carriers for glioblastoma treatment: An in vitro study, Cytotherapy 19 (2017) 721-734.
38. A. Benetti, A. Berenzi, M. Gambarotti, E. Garrafa, M. Gelati, E. Dessy et al, Transforming growth factor-beta1 and CD105 promote the migration of hepatocellular carcinoma-derived endothelium, Cancer Res 68 (2008) 8626-8634.
39. F. Pastorino, C. Brignole, D. Marimpietri, M. Cilli, C. Gambini, D. Ribatti, et al., Doxorubicin-loaded Fab' fragments of anti-disialoganglioside immunoliposomes selectively inhibit the growth and dissemination of human neuroblastoma in nude mice, Cancer Res 63 (2003) 7400-7409.
40. A. Bonomi, N. Steimberg, A. Benetti, A. Berenzi, G. Alessandri, L. Pascucci, et al., Paclitaxel-releasing mesenchymal stromal cells inhibit the growth of multiple myeloma cells in a dynamic 3D culture system, Hematol Oncol 35 (2017) 693–702.
41. D. Belotti, V. Vergani, T. Drudis, P. Borsotti, M.R. Pitelli, G. Viale, et al., The microtubule-affecting drug paclitaxel has antiangiogenic activity, Clin Cancer Res 2 (1996) 1843–1849.
42. R. Kinoshita, Y. Ishima, V.T.G. Chuang, H. Nakamura, J. Fang, H. Watanabe, et al., Improved anticancer effects of albumin-bound paclitaxel nanoparticle via augmentation of EPR effect and albumin-protein interactions using S-nitrosated human serum albumin dimer, Biomaterials 140 (2017) 162-169.
43. S.J. Clarke, L.P. Rivory, Clinical pharmacokinetics of docetaxel, in Clin Pharmacokinet, vol. 36, nº 2, pp. 99–114, 1999.
44. J.L. Eiseman, N.D. Eddington, J. Leslie, C. MacAuley, D.L. Sentz, M. Zuhowski, et al., Plasma pharmacokinetics and tissue distribution of paclitaxel in CD2F1 mice, Cancer Chemother Pharmacol 34 (1994) 465-71.
45. K.R. Aigner, F.O. Stephens, Induction Chemotherapy: Integrated Treatment Programs for Locally Advanced Cancer, Springer Science & Business Media, New York, 2011.
46. K.R. Aigner, S. Gailhofer, S. Kopp, Regional versus systemic chemotherapy for advanced pancreatic cancer: a randomized study, Hepatogastroenterology 45 (1998) 1125-1129.
47. Y. Zhang, Z. Guo, Z. Cao, W. Zhou, Y. Zhang, Q. Chen, et al., Endogenous albumin-mediated delivery of redox-responsive paclitaxel-loaded micelles for targeted cancer therapy, Biomaterials 183 (2018) 243-257.

48. X. Chen, Q. Wang, L. Liu, T. Sun, W. Zhou, Q. Chen, et al., Double-sided effect of tumor microenvironment on platelets targeting nanoparticles, Biomaterials 183 (2018) 258-267
49. M.G. Scioli, S. Artuso, C. D'Angelo, M. Porru, F. D'Amico, A. Bielli, et al., Adipose-derived stem cell-mediated paclitaxel delivery inhibits breast cancer growth, PLoS One 13 (2018) e0203426.
50. Pessina A., Leonetti C., Artuso S., Benetti A., Dessy E., Pascucci L. et al, Drug-releasing mesenchymal cells strongly suppress B16 lung metastasis in a syngeneic murine model. J Exp Clin Cancer Res 13 (2015) 82.
51. N. Priya, S. Sarcar, A.S. Majumdar, S. SundarRaj, Explant culture: a simple, reproducible, efficient and economic technique for isolation of mesenchymal stromal cells from human adipose tissue and lipoaspirate, J Tissue Eng Regen Med 8 (2014) 706-716.
52. J.H. Kim, Y. Kim, K.H. Bae, T.G. Park, J.H. Lee, K. Park, Tumor-Targeted Delivery of Paclitaxel Using Low Density Lipoprotein-Mimetic Solid Lipid Nanoparticles, Mol Pharmaceutics 12 (2015) 1230−1241.
53. X. Sheng, J.H. Parmentier, J. Tucci, H. Pei, O. Cortez-Toledo, C.M. Dieli-Conwright, et al., Adipocytes Sequester and Metabolize the Chemotherapeutic Daunorubicin, Mol Cancer Res 15 (2017) 1704-1713.
54. X. Sheng, J. Tucci, J.H. Parmentier, L. Ji, J.W. Behan, N. Heisterkamp, et al., Adipocytes cause leukemia cell resistance to daunorubicin via oxidative stress response, Oncotarget 7 (2016) 73147-73159.
55. E. Orgel, N.M. Mueske, R. Sposto, V. Gilsanz, D.R. Freyer, S.D. Mittelman, Limitations of body mass index to assess body composition due to sarcopenic obesity during leukemia therapy, Leuk Lymphoma 59 (2018) 138-145.
56. S.D. Mittelman, E. Orgel, Adipocyte metabolism of the chemotherapy daunorubicin, Oncoscience 5 (2018) 146-147.
57. L. Gille, H. Nohl, Analyses of the molecular mechanism of adriamycininduced cardiotoxicity, Free Radic Biol Med 23 (1997) 775–782.
58. M. Benguigui, D. Alishekevitz, M. Timaner, D. Shechter, Z. Raviv, S. Benzekry, et al., Dose- and time-dependence of the host-mediated response to paclitaxel therapy: a mathematical modeling approach, Oncotarget 9 (2017) 2574-2590.
59. D.A. Banyard, V. Borad, E. Amezcua, G.A. Wirth, G.R. Evans, A.D. Widgerow, Preparation, Characterization, and Clinical Implications of Human Decellularized Adipose Tissue Extracellular Matrix (hDAM): A Comprehensive Review, Aesthet Surg J 36 (2017) 349–357.

60. P.M. Crapo, T.W. Gilbert, S.F. Badylak, An overview of tissue and whole organcellularization processes, Biomaterials 32 (2011) 3233-3243.
61. L.E. Flynn, The use of decellularized adipose tissue to provide an inductive microenvironment for the adipogenic differentiation of human adipose-derived stem cells, Biomaterials 31 (2010) 4715-4724.
62. Y. Cheng, C. He, J. Ding, C. Xiao, X. Zhuang, X. Chen, Thermosensitive hydrogels based on polypeptides for localized and sustained delivery of anticancer drugs, Biomaterials 34 (2013) 10338-10347.
63. S.H. Kim, J.P. Tan, K. Fukushima, F. Nederberg, Y.Y. Yang, R.M. Waymouth, et al., Thermoresponsive nanostructured polycarbonate block copolymers as biodegradable therapeutic delivery carriers, Biomaterials 32 (2011) 5505-5514.
64. A.B. Dhanikula, R. Panchagnula, Development and characterization of biodegradable chitosan films for local delivery of paclitaxel, AAPS J 6 (2004) 88-99.
65. S.E. Kane, I. Pastan, M.M. Gottesman, Genetic basis of multidrug resistance of tumor cells, J Bioenerg Biomembr 22 (1990) 593–618.
66. L. Ge, X. You, J. Huang, Y. Chen, L. Chen, Y. Zhu, et al., Human Albumin Fragments nanoparticles as PTX Carrier or Improved Anti-cancer Efficacy, Front Pharmacol 9 (2018) 582.
67. Q. Xing, K. Yates, M. Tahtinen, E. Shearier, Z. Qian, F. Zhao, "Decellularization of fibroblast cell sheets for natural extracellular matrix scaffold preparation," in Tissue Engineering—Part C: Methods, vol. 21, no. 1, pp. 77–87, 2015.
68. E. Garrafa, G. Alessandri, A. Benetti, D. Turetta, A. Corradi, A.M. Cantoni, E. Cervi, A. Bonardelli, E. Parati, S.M. Giulini, B. Ensoli, A. Caruso, Isolation and characterization of lymphatic microvascular endothelial cells from human tonsils, J Cell Physiol 207 (2006) 107–113.
69. J.D. Gregory, S.W. Sajdera, Interference in the Lowry method for protein determination. Science 169 (1970) 97-98.

Figure legends

Figure 1

MFAT and DMFAT loaded with PTX displayed a potent anti-cancer activity on CFPAC-1

To evaluate anti-cancer activity, CFPAC-1 a human pancreatic cancer cell line was used. Different volume (from 25 µl to 200 µl) of MFAT **(A)** and DMFAT **(B)** loaded or not with 2 µg/ml PTX

were seeded in wells and co-cultured with CFPAC-1 placed in the upper compartment of trans-well inserts. Both MFAT-PTX and DMFAT-PTX strongly inhibited the growth of CFPAC-1 at all dose used even at lowest dose of 25µl. Controls not-primed MFAT and DFAT did not affect CFPAC-1 growth. In **(C)** is shown the effect of 25 µl of both MFAT-PTX and DMFAT-PTX evaluated by using colorimetric assay. In **(D)** MFAT-PTX and **(E)** DMFAT-PTX effect on CFPAC-1 proliferation investigated by MTT assay. Different dose (from 25 µl to 200 µl) of MFAT-PTX and DMFAT-PTX specimens were cultured for 24h and CM was added to CFPAC-1 at scalar dilutions. In **(F)** the p-EC values corresponding to the PTX released in the CM by either MFAT-PTX and DMFAT-PTX. A high correlation between p-EC values and the dose of MFAT-PTX or DMFAT-PTX used, but no significant differences ($p>0.05$) were found. Columns and values in the figures are the means ± SD of three separate experiments, performed in triplicate. *t*-test: °° indicate $p<0.01$ versus CTRL medium**;** and ** $p<0.001$ versus CTRL MFAT and DMFAT derived CM.

Figure 2

MFAT and DMFAT loaded with different PTX concentrations displayed a dose-dependent anti-cancer activity on human NB and GBM cancer cells

In **(A)** and **(B)** the anti-proliferative activity of CM from MFAT-PTX and DMFAT-PTX (loaded with 2 µg/ml), tested at different dilutions (1.2 to 1:8) on human IMR-32 (NB) and U87MG (GBM) cancer cells respectively. In **(C)** and **(D)** representative images of IMR-32 and U87MG cancer cell cultures upon 72h treatment with CM (1:2 dilution) from MFAT-PTX and DMFAT-PTX respectively (photos 10x magnifications). Photographs shown the potent anti-cancer activity of CM from MFAT-PTX and DMFAT-PTX and the presence of several necrotic cancer cells.
CM from MFAT-PTX **(E)** and DMFAT-PTX **(F)** primed with different PTX concentration produced a dose dependent growth inhibition.
To note, CM recovered from both MFAT and DMFAT primed with PTX at 0.125 µg/ml was not effective. Columns in the figures are the means ± SD of two separate experiments, done in triplicate. *t*-test: * indicate $p<0.05$; ** $p<0.01$ versus CTRL MFAT and DMFAT derived CM respectively.

Figure 3

MFAT-PTX and DMFAT-PTX showed a potent in vitro anti-angiogenic activity

In **(A)** HUVECs were cultured for 72 h in the presence of different dilution of CM derived from MFAT-PTX, DMFAT-PTX (2µg/ml) and control unprimed specimens. CM from both MFAT-PTX and DMFAT-PTX, at all dilutions tested, significantly inhibited HUVECs proliferation.

Similar results were obtained by co-culturing in tras-wells HUVECs with different amount of DMFAT-PTX **(B).** In **(C)** photographs of HUVECs treated with CM (1:2 dilution) from control and PTX primed MFAT and DMFAT specimens. Cells were fixed and stained after 72h treatment. Arrows indicate the ECs with nuclear fragmentation, an apoptotic feature that was particularly induced by CM from DMFAT-PTX

Columns in the figures are the means ± SD of three separate experiments, done in triplicate. *t*-test: °° indicate $p<0.01$ versus EGM control medium; **$p<0.01$ vs control MFAT and DMFAT specimens.

Figure 4

In vitro long lasting anti-cancer activity of MFAT-PTX and DMFAT-PTX specimens and kinetics of PTX release.

In **(A)** and **(B)** is shown CFPAC-1 growth inhibition of serial dilutions of CM derived from MFAT-PTX and DMFAT-PTX(2µg/ml) recovered upon different time of incubation (from 1 to 7 days), respectively. CM was aspirated and replaced with fresh medium at each time tested. The kinetics of PTX released from MFAT-PTX and DMFAT-PTX is shown in **(C)** and **(D)**, respectively. To note, the PTX released by DMFAT-PTX, expressed as p-EC, was around double compared to p-EC released by MFAT-PTX. The total PTX released during the first week from DMFAT-PTX was 15,1% and from MFAT-PTX was 8.75% of the total loaded. In **(E)** and **(F)** long lasting anti-cancer activity against U87MG and IMR-32 of both MFAT-PTX and DMFT-PTX derived CM is shown. To note, even after 8 weeks, U87MG and IMR-32 proliferation was still significantly inhibited. In (**F**) and (**H**) the kinetics of PTX released every week (for 8 weeks) by MFAT-PTX and DMFAT-PTX expressed as p-EC. In summary, p-EC released by DMFAT-PTX was about double of that released by MFAT-PTX, at each time investigated. After 8 weeks of culture, the percentage of p-EC released by MFAT-PTX and DMFAT-PTX was about 40% and 80% of the total PTX initially loaded respectively. Columns and numbers in the figure are the means ± SD of two separate experiments, done in triplicate. *t*-test: ° indicates $p<0.05$; °° $p<0.01$ versus p-EC released by MFAT-PTX; * indicate $p< 0.05$; **$p<0.01$ vs CM of control MFAT and DMFAT specimens.

Figure 5

PTX timing of uptake, localization and release by MFAT and DMFAT specimens.

To evaluate the time necessary for drug uptake by MFAT and DMFAT, specimens were treated with 2 µg/ml of PTX for 5' to 24h. In **(A)** the values of PTX, expressed as p-EC, unbound and

bound to MFAT or DMFAT specimens upon 5' are reported. To note, 5' was sufficient to incorporate about all the drug (95% MFAT and 90% DMFAT) added. In **(B)** photographs (10x magnification) showing morphological appearance and localization of PTX-F35 in live MFAT and DMFAT specimens are reported. The adipocytes cell component of both MFAT and DMFAT was able to incorporate most of PTX-F35 added that was also found in the SVF of MFAT but was almost completely absent in SVF of DMFAT. CM from DMFAT-PTX and MFAT-PTX at 24h was analyzed by HPLC. The elution profile **(C)** was compared to that of pure PTX at 1.000 ng/ml **(D)**. The figure reports a chromatogram profile of one typical experiment where CM from DMFAT-PTX evidences a peak that clearly identified PTX based on a PTX standard curve. Numbers in the figure are the means ± SD of three separate experiments, done in triplicate.

Figure 6

Anti-tumor effects of DMFAT-PTX in an orthotopic animal model of human NB

In **(A)** nude mice (n = 5/group) were injected with 1×10^6 HTLA-230 cells in the left adrenal gland (d_0) and then treated, at the days reported (T_{1-4}), either i.p. or i.v. with 10 mg/kg of DMFAT-PTX and free PTX, respectively. Control (CTRL) mice received saline. In the figure the survival of the mice bearing HTLA-230 was not affected by the systemic treatments of either free PTX or DMFAT-PTX.

In **(B)** BLI of primary tumor re-growth after surgical resection of orthotopically implanted HTLA-230-luc human NB cells**.** Mice were treated after tumor resection and at the days reported (T_{1-5}) with 10 mg/kg of either DMFAT-PTX or free PTX. Control (CTRL) mice received saline. BLI was performed 2h after tumor resection (d_{18}) and 24h after the last treatment (d_{41}). Although systemic free PTX and local DMFAT-PTX treatments were both effective on HTLA-230-luc relapse (no statistical difference $p > 0.05$), BLI in the mice treated with DMFAT-PTX was not detected until day 41 when the mice were sacrificed.

In **(C)** BLI of primary tumor re-growth after surgical resection of orthotopically implanted IMR-32-luc cells (d_0) is shown. Tumors were surgically resected on day 14 (d_{14}) and mice were initially treated after tumor resection with 15 mg/kg of either DMFAT-PTX or free PTX in loco and i.v., respectively. Since 69% free PTX-treated mice and 21% DMFAT-PTX mice died for toxicity and for respiratory problems after 48h from treatments respectively, only a second treatment was repeated reducing PTX dose at 10 mg/kg. BLI was performed after tumor resection (d_{14}) and at d_{22}. Both treatments were very effective to reduce IMR-32-luc relapse. Columns in the figures are the means ± SD; $^{**}p<0.01$ vs control mice treated with saline.

Figure 7

PK of PTX released by DMFAT-PTX in vivo

In **(A)** are shown the blood concentrations of PTX released by DMFAT-PTX (200µl/10mg/kg) given (i.p.) or (s.c.) and detected at 2, 24, 72 and 168h after injection. As expected, at 2h, the plasmatic concentration of PTX after s.c. treatment was significantly lower (14%) than when i.p. injected. The values of the apparent volume of distribution at 2h (Vd_{2h}) were 105,2 ml (i.p.) and 716,8 ml (s.c.). Therefore, subcutaneous localization of DMFAT-PTX showed a better bio-distribution in tissues compared to systemic i.p. injection. In **(B)** are shown the organ concentrations and residual amount of drug values in the site of subcutaneous injection. To note**,** at 2h PTX measured in liver and kidney was significantly higher when the drug was inoculated i.p. than when s.c. administered. When DMFAT-PTX was given s.c. the bioavailability of PTX in liver and kidney was reduced of 73 % and of 86 % respectively. The residual amount of PTX found in situ after 2h was about 50 % of those injected, but after 168h the drug in the residual DMFAT specimens (up to 3 µg/gr) must be considered of pharmacological importance. In **(C)** the area under the curve (AUC) values are reported. In summary the values of AUC for plasma and two organs was lower if DMFAT-PTX was given s.c. To note, the AUC of residual amount of PTX after s.c. treatment was 2452 time higher than that found for plasma. Numbers in the figures are the means ± SD.

Figure 1

Click here to download high resolution image

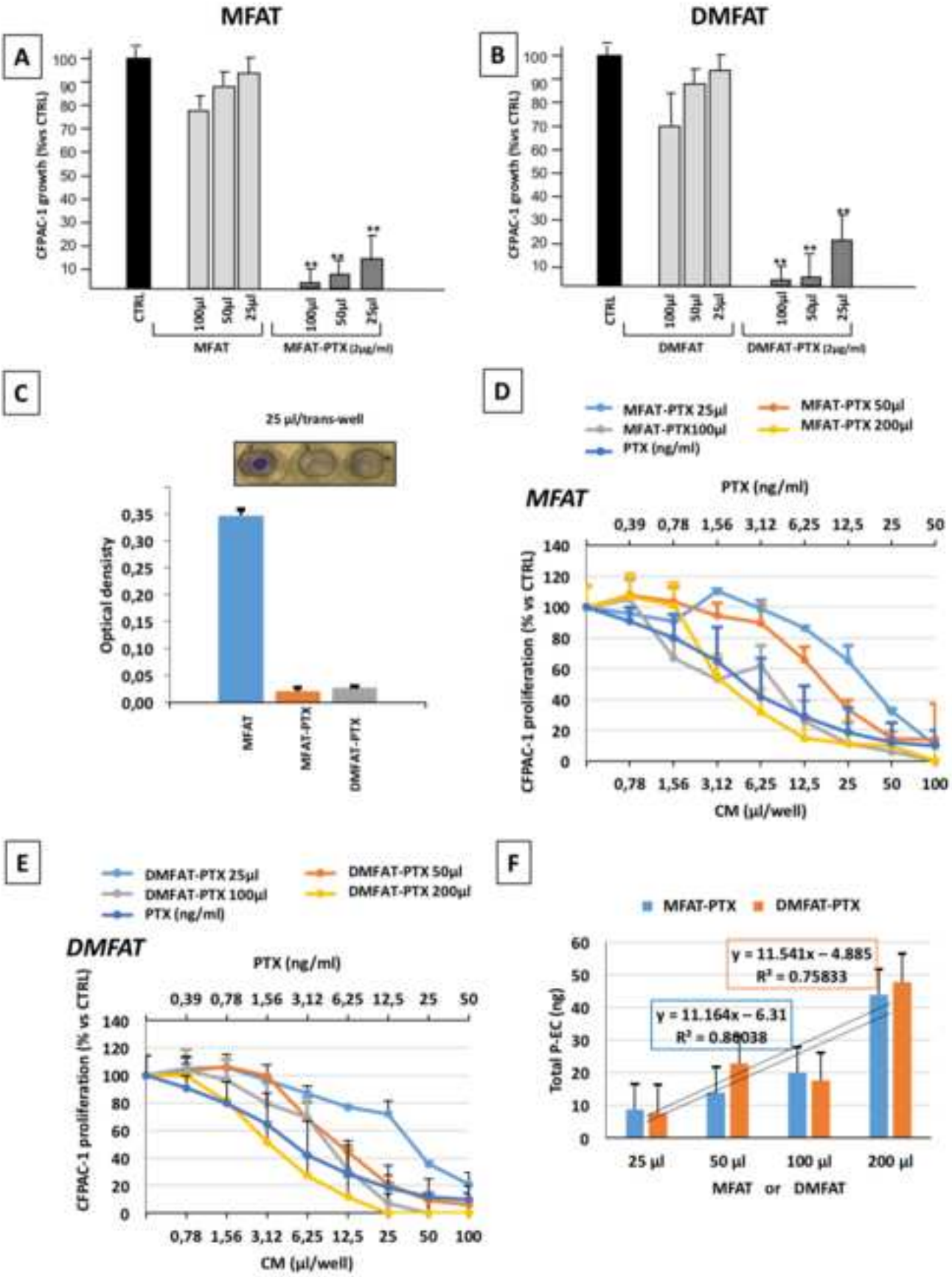

Figure2

Click here to download high resolution image

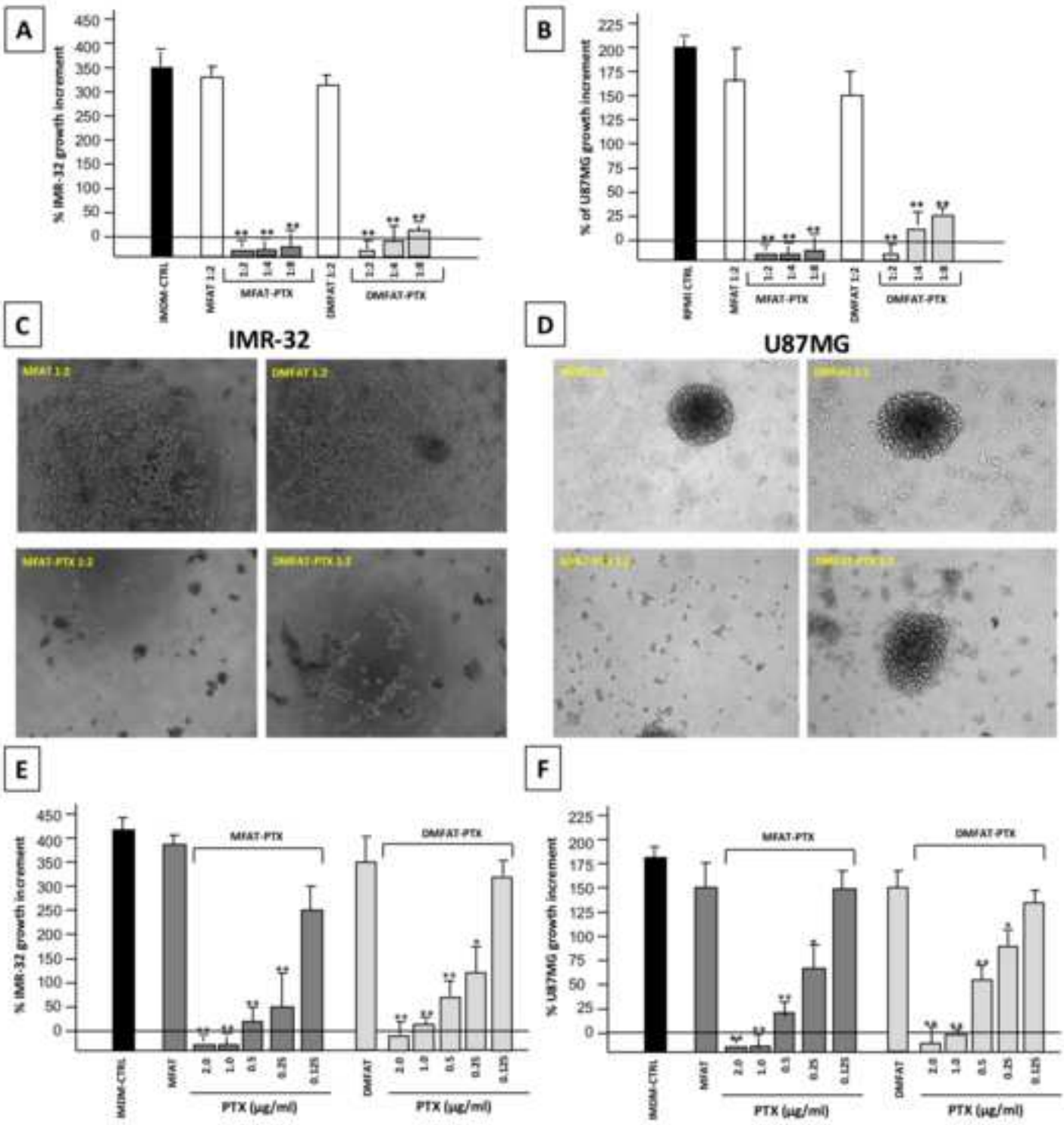

Figure3

Click here to download high resolution image

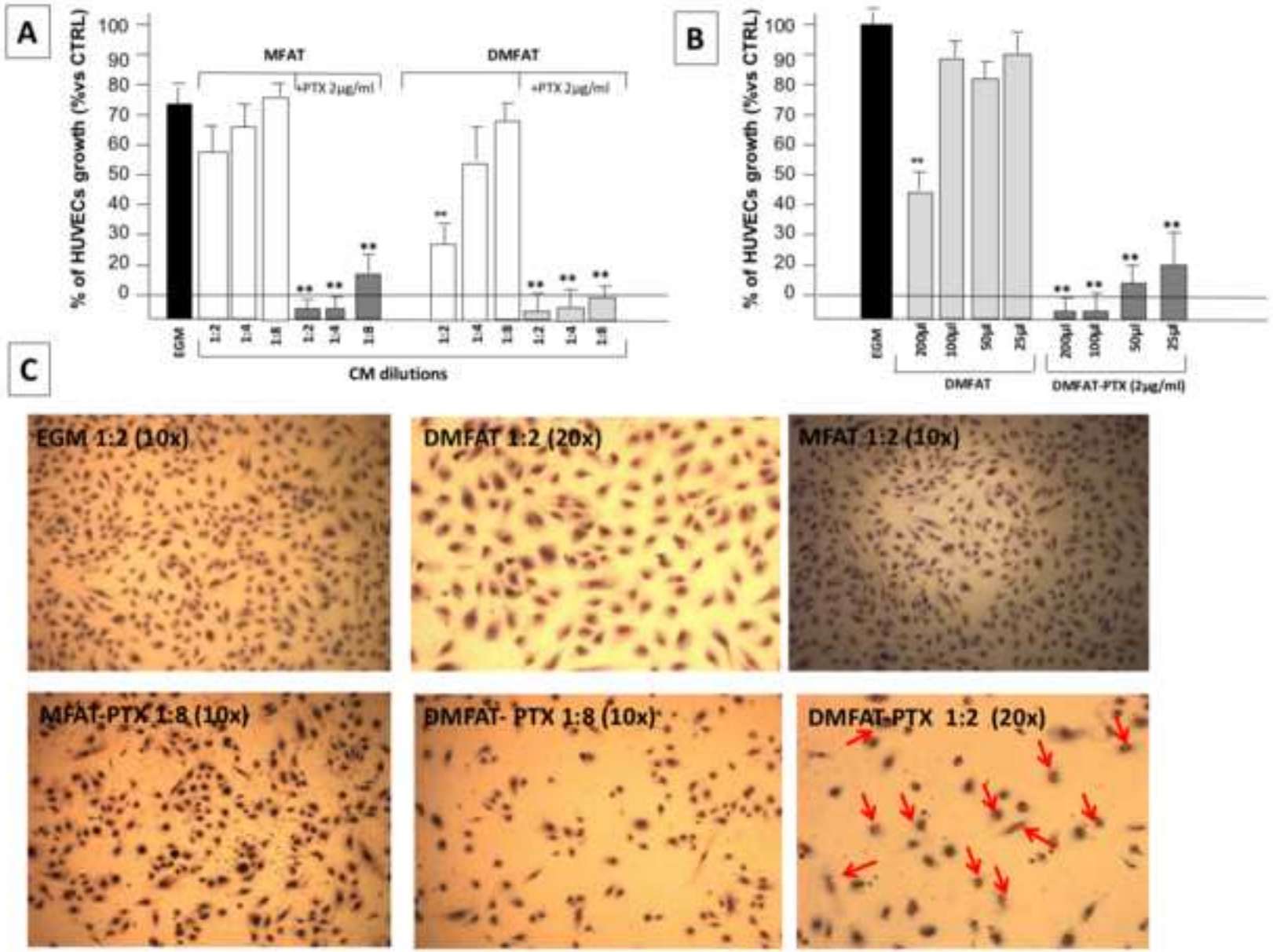

Figure4

Click here to download high resolution image

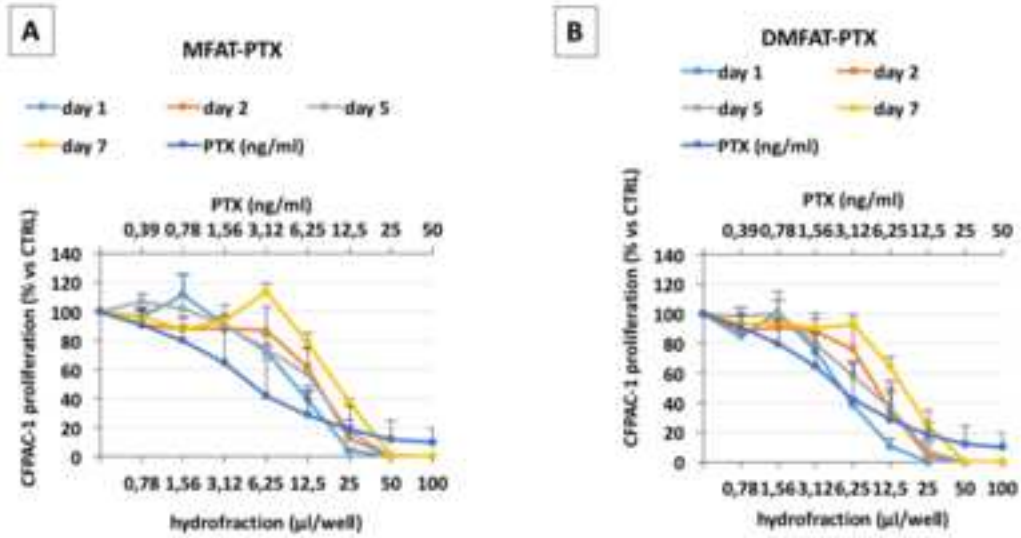

C

MFAT-PTX	Day 1	Day 2	Day 5	Day 7
Total p-EC (ng/ml)				
P-EC accumulation (ng/ml)				
% of PTX release				

D

DMFAT-PTX	Day 1	Day 2	Day 5	Day 7
Total p-EC (ng/ml)				
P-EC accumulation (ng/ml)				
% of PTX release				

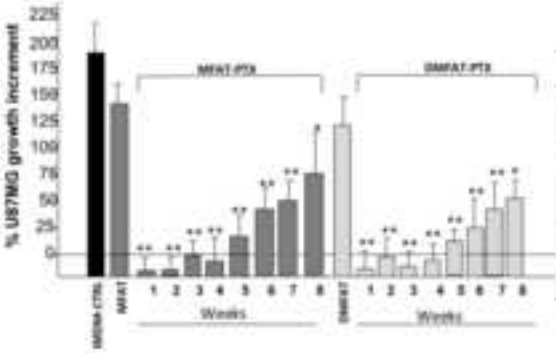

F

	Weeks							
MFAT-PTX	1	2	3	4	5	6	7	8
P-EC (ng/ml)								
Totale p-EC (ng/ml)								
% of PTX release								

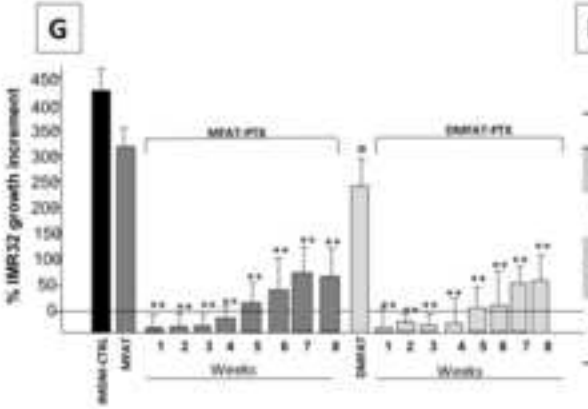

H

	Weeks							
DMFAT-PTX	1	2	3	4	5	6	7	8
P-EC (ng/ml)								
Totale p-EC (ng/ml)								
% of PTX release								

Figure5

Click here to download high resolution image

A

MFAT-PTX	MFAT-PTX (5')	DMFAT-PTX (5')
Unbound Total p-EC (ng/ml)	104.56 ± 49.89	201.55 ± 11.78
Unbound PTX (%)	5.22 ± 1.57	10.00 ± 3.49
Bound PTX (%)	94.78 ± 4.05	90.00 ± 5.58

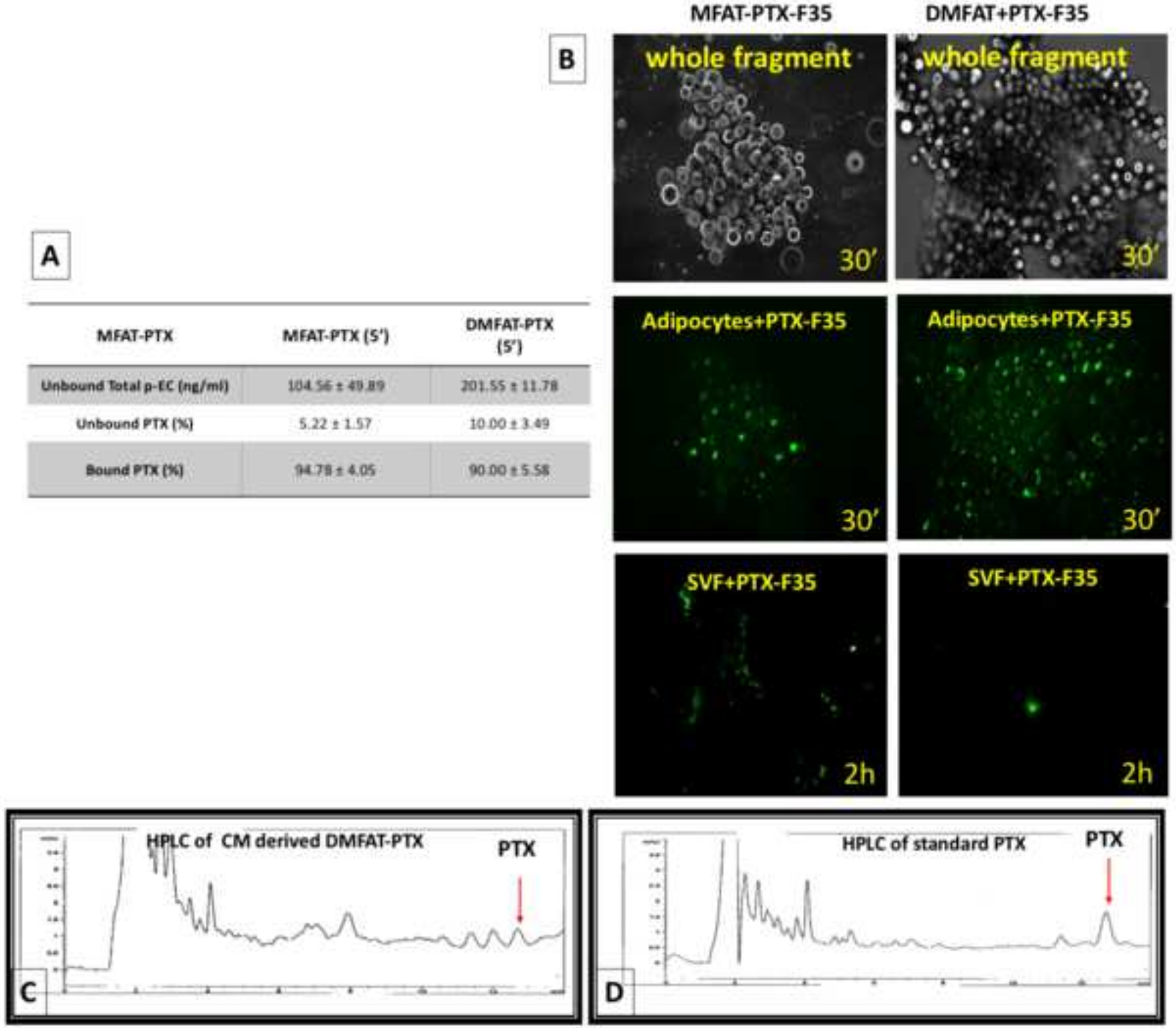

Figure6

Click here to download high resolution image

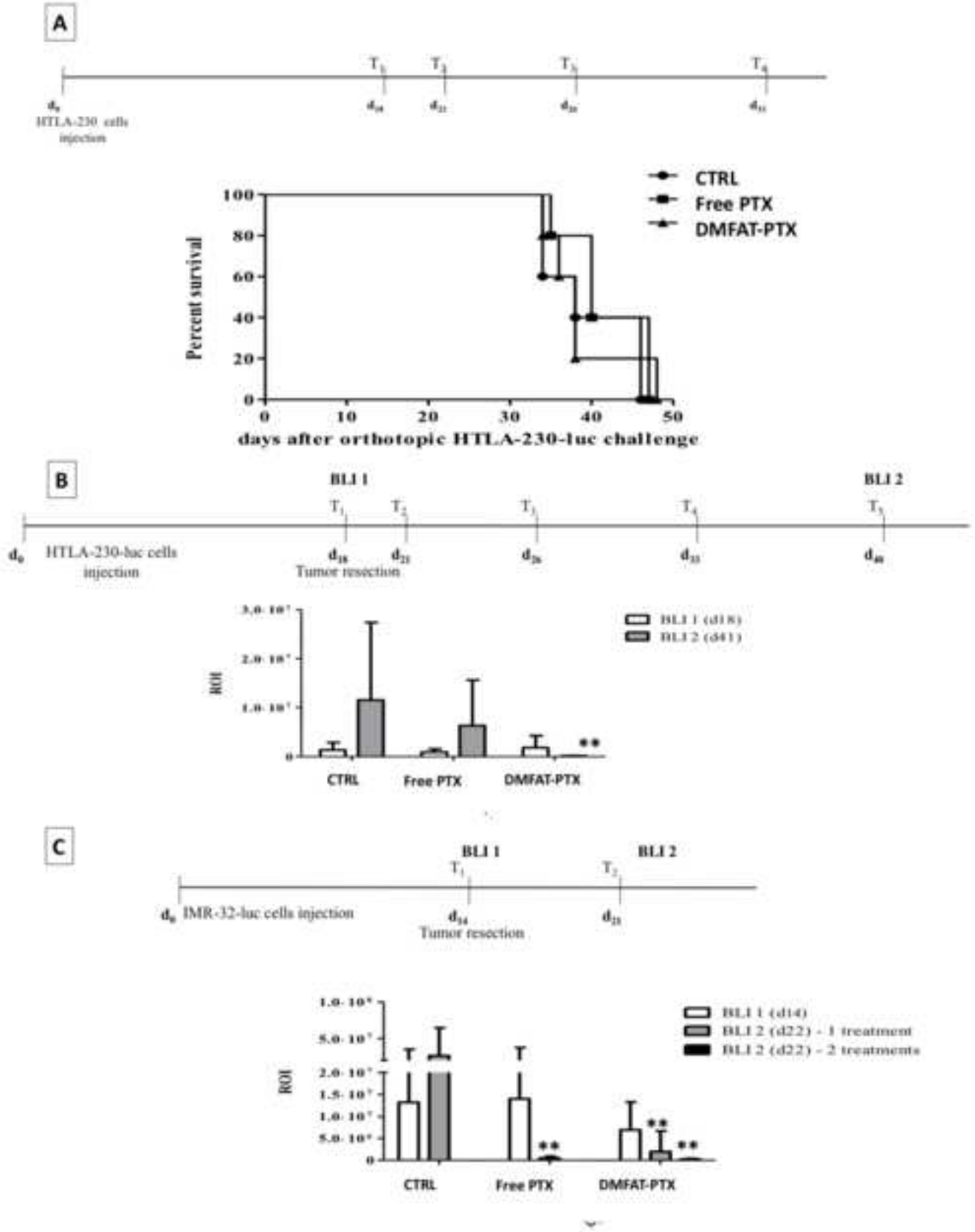

Figure7

Click here to download high resolution image

A

Blood concentration

I.P.: Plasma (µg/ml)			
2 hours	24 hours	72 hours	7 days
1.90± 0.94	0.004± 0.002	0.003 ± 0.001	0.01 ± 0.02

I.P. Vd $_{2h}$ = 105.2 ml

S.C.: Plasma (µg/ml)			
2 hours	24 hours	72 hours	7 days
0.27 ± 0.05	0.01 ± 0.009	0.004 ± 0.003	0.002 ± 0.0006

S.C. Vd $_{2h}$ = 716.8 ml

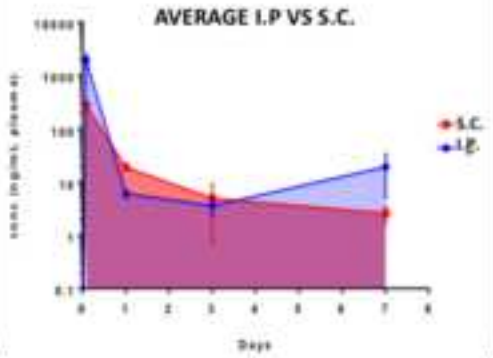

B

Organ concentration

µg/g	2 hours	24 hours	72 hours	7 days
I.P.: liver	45.90 ± 10.32	0.40 ± 0.02	0.15 ± 0.07	0.34 ± 0.14
S.C.: liver	12.35 ± 3.00	0.14 ± 0.05	0.17 ± 0.07	1.36 ± 0.30
I.P.: kidney	26.54 ± 5.15	0.83 ± 0.35	1.34 ± 0.55	0.17 ± 0.05
S.C.: kidney	3.84 ± 0.40	0.20 ± 0.08	0.08 ± 0.03	0.06 ± 0.03

Residual amount in situ after s.c. injection

µg/gr			
2 hours	24 hours	72 hours	7 days
490.75 ± 161.01	49.63 ± 9.21	18.00 ± 12.46	3.13 ± 1.65

C

Area under the curve (AUC)

Pharmacokinetic	AUC (total µg/days)
I.P. plasma	0.98
I.P. liver	15.24
I.P. kidney	4.20
S.C. plasma	0.16
S.C. liver	5.91
S.C. kidney	0.69

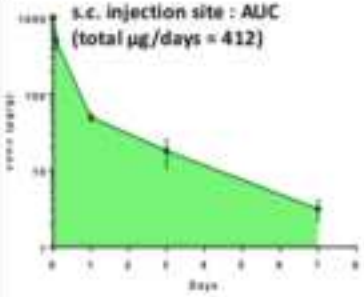

Supplementary Material

Click here to download Supplementary Material: Supplementary Figures Legend_revision.docx

Supplementary Material

Click here to download Supplementary Material: Supplementary Figures_revision.pptx

Highlights

Click here to download Supplementary Material: Highlights.docx

Supplementary Material

Click here to download Supplementary Material: Supplementary Material and Methods_revision.docx

Supplementary Material

Click here to download Supplementary Material: Supplementary Tables_revision.pptx